NASA DEVELOP National Program
Alabama – Marshall
Summer 2021

Delaware Ecological Forecasting

Assessing Land Cover and Soil to Identify Suitable Sites for Tidal Marsh Migration in Delaware

DEVELOP Technical Report
Final Draft – August 12th, 2021

McKenna Brahler (Project Lead)
Amanda Bosserman
Eian Davis
Jacob Frankel
Rebecca Ohman

Advisors:
Dr. Robert Griffin (The University of Alabama in Huntsville)
Dr. Jeffrey Luvall (NASA Marshall Space Flight Center)

1. Abstract

Tidal wetlands provide vital resources for the state of Delaware, crucial not only for maintaining important ecosystem functions, but also for providing human populations with substantial services. Healthy wetland networks offer protection from severe weather, reduce flooding, improve water quality, and provide opportunities for education and recreation. However, human activities in combination with natural events, continue to cause substantial loss of wetland cover and damage wetland health. Over the last thirty years, the state of Delaware has experienced a net loss of roughly 5,000 acres of wetland. In collaboration with the Delaware Department of Natural Resources and Environmental Control (DNREC), the team used NASA Earth observations including Landsat 5 Thematic Mapper (TM), Landsat 8 Operational Land Imager (OLI), Terra Moderate Resolution Imaging Spectroradiometer (MODIS), and Global Precipitation Measurement Integrated Multi-Satellite Retrievals (GPM IMERG) to develop a methodology to monitor recent changes in wetland cover and forecast landward marsh migration due to sea-level rise, changes to climate, and human development. Trend analysis of current and past climate conditions in precipitation and temperature revealed an overall increase in both metrics. Using Land Change Modeler in TerrSet and Suitability Modeler in ArcGIS Pro, the team visualized landcover shifts over the last 20 years, indicating a general pattern of net wetland loss and identified locations where marsh migration could potentially occur in the future. These observations will enable better planning for restoration activities and inform decision-making to preserve wetland health and ecosystem functions.

Key Terms

Delaware, coastal wetlands, remote sensing, Land Change Modeler, Landsat, sea-level rise

2. Introduction

2.1 Background Information

Tidal wetlands are an integral part of Delaware's coastal ecology, providing numerous ecosystem services and direct economic and societal benefits to the state. Tidal wetlands include a variety of aquatic environments such as freshwater tidal marsh, salt marsh, and brackish marsh. These wetlands aid in carbon sequestration and water purification, while simultaneously providing habitat for native species, protection against storm surges, and opportunities for recreation (Barbier et al. 2011). Over the last few decades, this important resource has been under tremendous stress from increasing human activity and sea-level rise (SLR). According to the Department of Natural Resources and Environmental Control (DNREC), Delaware has lost approximately 5,000 acres of its wetlands in the last thirty years due to residential development and conversion to agriculture (Tiner et al. 2011). In 2006, stressors from high densities of human population, specifically along the coastal region of Delaware, showed a correlation with sudden wetland dieback (SWD) in salt marsh wetland habitat (Rogerson et al. 2009). While significant wetland loss is due to land reclamation, wetland stresses are likely to become aggravated by shifts in climate and SLR rates (Blankespoor et al. 2014). The study area for this project is the state of Delaware, with an emphasis on the coastal region. This study examined wetland migration trends over the previous decade (2010-2020), projected those trends to the year 2050, and analyzed current patterns for marshland habitat. Prior wetland classification studies have

demonstrated the benefits of using satellite imagery in combination with Digital Elevation Models (DEM) and high spatial resolution aerial photography for classifying wetland types, among other landcover classes (Lamb et al. 2019; Wang et al. 2019). Satellite imagery, though varying in spatial and temporal resolution, can provide long-term documentation of marsh classification attributes, such as surface and soil hydrology and the presence of hydrophilic vegetation (Correll et al. 2018). Even using a combination of these data sources, classifying wetlands remotely remains a challenge. Supervised classification using the Random Forest (RF) machine learning algorithm for wetland classification showed the most promise in terms of accuracy, efficiency, and ease of use with our intended datasets, with an accuracy over 85% when used to classify Landsat 8 Operational Land Imager (OLI) data in a coastal wetland study (Wang et al. 2019). The use of RF machine learning allowed the team to analyze large, complex datasets to best understand the current conditions of Delaware's coastal wetlands and forecast trends for future restoration strategies.

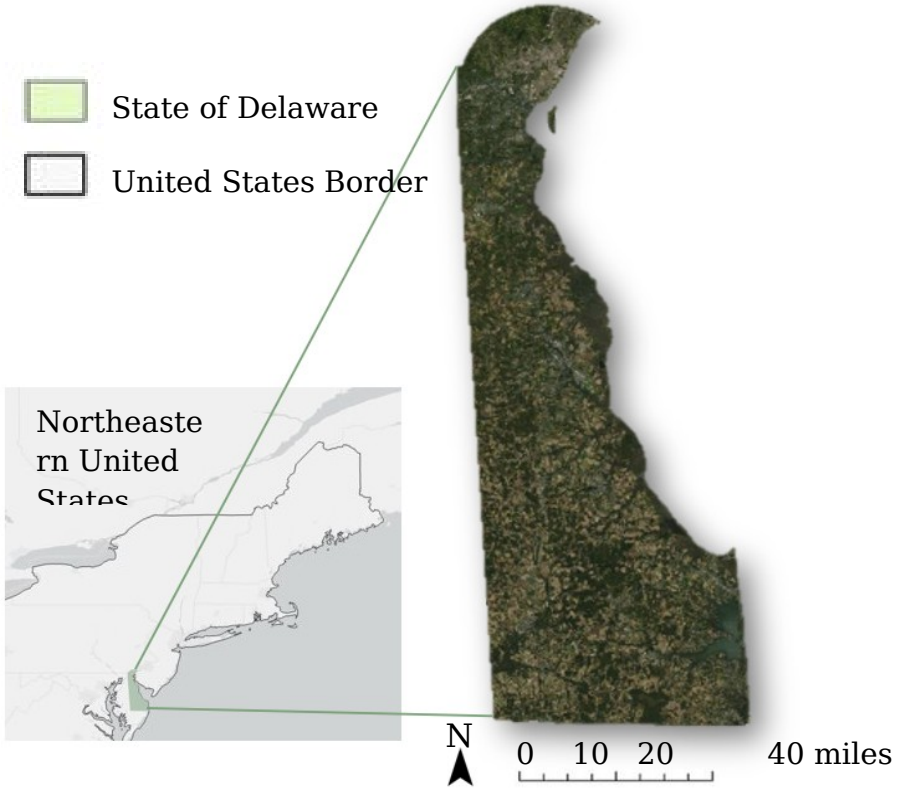

Figure 1. Study area map depicting the state of Delaware in the Northeastern United States.

2.2 Project Partners & Objectives

The partner for this project was DNREC, an organization that aims to protect public health and the environment of the state of Delaware while providing areas for outdoor recreation. DNREC also leads the energy policy and climate preparedness for the state in addition to educating the public on historical, cultural, and natural resource use importance. DNREC was specifically interested in this project due to the growing concern of wetland habitat loss and tidal marsh migration occurring along Delaware's coast. The data and information provided by

this project will assist DNREC in making decisions about where to focus on marsh migration efforts and wetland expansion projects.

This project had four main objectives. The first was to identify current and future wetland habitats, marsh locations, and changing climate variables. Using these observations, the team analyzed LULC (Land Use Land Cover) change and marsh migration over the past decade, as well as climate variable trends since 2000. Next, the team generated maps of wetland habitat and marsh locations during the study period. Finally, these maps were used to predict areas of likely landward marsh migration in different land cover change scenarios. The team provided a thorough methodology for DNREC to use in the future to create similar end products.

3. Methodology

3.1 Data Acquisition

3.1.1 Land Use Land Cover Change

The team used surface reflectance data from Landsat 5 Thematic Mapper (TM), Landsat 8 OLI, and aerial photography from National Agriculture Imagery Program (NAIP, Table 1). To obtain Landsat imagery, image collections for the 2010 (Landsat 5 TM) and 2020 (Landsat 8 OLI) date ranges were loaded through Google Earth Engine (GEE), and pixels averaged across images from April through August. The same process was repeated with NAIP imagery for the year 2018. For the forecasting portion of the LULC analysis, the team compiled additional data from Delaware's FirstMap website for use in TerrSet's Land Change Modeler (LCM). Layers of statewide elevation from a DEM and roads were incorporated in both the change analysis and forecasting modules, and the team used a 2019 map of Public Protected Lands for some forecasting models.

Table 1
Data used for the Land Use Land Change Models

Satellite & Sensor	**Earlier Image Date**	**Later Image Date**	**Data Source**
Landsat 5 TM	04/01/2010 - 08/31/2010	N/A	GEE, Collection 1 Tier 1 Surface Reflectance
Landsat 8 OLI	N/A	04/01/2020 - 08/31/2020	GEE, Collection 1 Tier 1 Surface Reflectance
NAIP	N/A	04/01/2018 - 08/31/2018	GEE, USDA Farm Production and Conservation

3.1.2 Tidal Marsh Suitability

The team used five criteria to assess the locations of suitable land for tidal marsh migration and conservation efforts. The impervious descriptor band was downloaded from the USGS National Land Cover Database using GEE to create the impervious surfaces criterion. The team used a DEM from Delaware's FirstMap website to create a measure of slope, and hydrological data from the USGS National Hydrology Dataset to identify water availability. To identify hydric soils, the team obtained soil data created by the National Cooperative Soil Survey from

Delaware's FirstMap website. To identify land unavailable to marsh migration due to the presence of agricultural crops, the team accessed cropland data from the USDA National Agricultural Statistics Service (NASS). More detailed information can be seen in Table 2.

Table 2
Data used in the Tidal Marsh Suitability Model

Data	**Data Use**	**Data Source**	**Dates Collected**
National Land Cover Database	The impervious descriptor band was downloaded from a land cover classification image; the layer represents all areas of Delaware that are covered with impervious surfaces	USGS National Land Cover Database downloaded from GEE	2016
Digital Elevation Model	DEM layer was used to create a measure of slope in degrees	Delaware's FirstMap website	Winter 2013/Spring 2014
National Hydrology Dataset Flowlines	Hydrology flowlines were used to identify areas with tidal influence and water connectivity	USGS National Hydrography Dataset plus high resolution from USGS website	August 13, 2018
Delaware Soils (downloaded by county)	Soil layers used to identify hydric soils indicative of marshland	Delaware's FirstMap website, developed by the National Cooperative Soil Survey	New Castle County (2015), Sussex County (2017), Kent County (2017)
Cropland	Layer taken from a land cover classification image; layer represents all areas of Delaware that are covered with agricultural land	Taken from the USDA NASS 2020 layer, designed to show crop distribution. Downloaded from GEE.	01/01/2020 - 12/31/2020

3.1.3 Climate Analysis
The team chose to use two different NASA Earth observations to create the climate analysis. The team selected the Global Precipitation Measurement Integrated Multi-Satellite Retrievals (GPM IMERG) Merged Satellite-Gauge Precipitation Estimate – Final Run (GPM_3IMERGM v06) to analyze potential seasonal precipitation variation between the years 2000 and 2020, and the Terra MODIS Monthly Daytime 3min CMG Land-surface Temperature dataset (MOD11C3) to investigate variation in seasonal temperature between the years 2000 and 2020. For statistical analysis, the team downloaded data from GEE; GPM was available

as monthly averages for the study period, while Terra MODIS data was available by 8-day average. Data and images from these Earth observations were downloaded from NASA EarthData and Giovanni. For map production, the team downloaded data in 5-year seasonal averages (2000-2005, 2005-2010, 2010-2015, 2015-2020). These datasets were chosen because of their relatively high spatial resolution (Table 3). Due to the small size of the state of Delaware, it was important to use higher resolution datasets to provide a clear analysis of climate variables.

Table 3
Data used for the Climate Analysis

Satellite & Sensor	**Earlier Image Date**	**Later Image Date**	**Data Source**	**Spatial Resolution**
Global Precipitation Measurement (GPM) Average Merged Satellite-Gauge Estimate Final Run Monthly	12/1999	11/2020	NASA EarthData, Giovanni	0.1°, latitude and longitude
Terra Moderate Resolution Imaging Spectroradiometer (MODIS) Land Surface Temperature/Emissivity Monthly	12/1999	11/2020	NASA EarthData, Giovanni	0.05°, latitude and longitude

3.2 Data Processing

3.2.1 Land Use Land Cover Change

To download clear Landsat images in GEE, the team used a cloud masking script to isolate pixels with no data from analysis. The April to August study dates were chosen to allow for substantial cloud-free data for masking. The team used the same process for the NAIP data, except no cloud masking was necessary, and 2018 was the most recent year for which NAIP imagery was available. Because NAIP imagery had such fine resolution (1 meter), the images often exceeded the GEE pixel limit. In response, the team aggregated pixels and exported the images at a resolution of 5 meters.

The LULC portion of the project included two parts: RF classification of wetlands in the earlier and later images, and change analysis and prediction of future land cover performed in TerrSet LCM. Because of the size of the images and time constraints, the team only conducted change analysis for the Landsat products. NAIP imagery was used to create a map of land cover as of 2018, but an earlier image was not created. To perform RF classification, the team created several ancillary images to use in concordance with the spectral bands from the satellite imagery. These ancillary images were created in ArcGIS Pro using the Raster Function suite of tools. Ancillary datasets were chosen based on the results of a 2019 study evaluating the accuracy of wetland remote sensing methods in China (Wang et al. 2019). Table 4 shows the bands used for each of the indices used. The team used ancillary data to produce Normalized Vegetation Difference Index

(NDVI), Soil Adjusted Vegetation Index (SAVI), Normalized Difference Water Index (NDWI), Normalized Difference Built Index (NDBI), and PCA components 1 and 2. The team transformed additional elevation, roads, and public protected lands data into raster images for LCM change analysis and forecasting.

Table 4
Due to the fact that NAIP only has Blue, Green, Red, and NIR bands, only the NDVI and SAVI indexes were created. The table below gives information about the bands from the different satellites used.

Region	**Landsat 5**	**Landsat 8**	**NAIP**
Red	Band 1	Band 2	Band 1
NIR (Near Infrared Region)	Band 4	Band 5	Band 4
SWIR (Short-Wave Infrared Region)	Band 5	Band 6	N/A

3.2.2 Tidal Marsh Suitability

The tidal marsh suitability analysis involved performing data processing steps on each of the five criteria. The team extracted the impervious surface layer from the USGS National Land Cover Database from 2016 in GEE. The impervious descriptor band was selected for analysis because it defined where impervious layer pixels are roads and provided the best fit description for impervious pixels that were not roads. After importing this data into ArcGIS Pro, the team clipped national impervious surfaces data to the state extent of Delaware, accessed from FirstMap. The team used the Build Raster Attribute Table tool to turn values for impervious classifications into an attribute table, and reclassified the value of all developed areas to 0 and all undeveloped areas to 1. All developed areas were considered to have the same weight.

The team acquired Delaware soils data by county, and merged the data into one layer with the Merge tool in ArcGIS Pro. This layer was then changed to a raster using the Polygon to Raster tool in order to be added to the Suitability Modeler. A measure of slope was created from DEM data using the slope tool. The Resample tool was used on the slope data to increase the resolution from 1 meter to 100 meters to improve processing time and avoid software overload. To identify agricultural land, the team downloaded the USDA National Agricultural Statistics Service Cropland Data layer using GEE. In ArcGIS Pro, the Reclassify tool was used to identify and isolate land used for agriculture from all other land use types. Agricultural land was reclassified as 1 and all other land was reclassified as 0.

Flowline data was downloaded from the USGS National Hydrography Dataset. The Euclidean Distance tool was used to determine the distance from sources of water like rivers and streams. Under the Environments tab in this tool, a mask of the Delaware state outline was used to exclude the Delaware bay. Without this mask option, the Euclidian Distance results were incorrect. Following these processing steps, all criteria were entered into the Suitability Modeler for analysis.

3.2.3 Climate Analysis

The team used three different methods of climate analysis to visualize and interpret trends from the GPM and Terra MODIS datasets. To perform these

methods, QGIS, GEE, and Microsoft Excel were all utilized. Terra MODIS data were averaged over a monthly time scale to match GPM monthly averages, and both datasets were exported as a comma-separated values (CSV) file for further analysis. Downloaded data were imported into QGIS and clipped to the bounds of the state of Delaware. For the seasonal climate analysis, temperature and precipitation records were categorized by seasonal month:

- Spring to March, April, May
- Summer to June, July, August
- Fall to September, October, November
- Winter to December (of the previous year), January, February (winter records listed as the year of the first month, December)

3.3 Data Analysis

3.3.1 Land Use and Land Cover Change

The team used two different methodologies for working with the Landsat and NAIP products. The Landsat products were classified using the Image Classification Wizard tool in ArcGIS Pro, while NAIP products were classified using a script in GEE, as the size of these images provided challenges working in ArcGIS tools. This also allowed the team to compare two RF classification methods. For the Landsat data, the team opted to use the Image Classification Wizard for its segmentation ability and ease of use. The team used a supervised classification approach along with the Object Based Image Analysis option. For both the earlier and later Landsat images, the following classes were chosen: Non-Wetland Vegetation/Open Space, Wetlands, Water, and Developed space. Non-Wetland Vegetation also included areas of forest, shrubland, and cropland. Around 20 to 25 segments were chosen in the Image Classification Wizard as training data for each class, located in close proximity for the early and later images. In the Train window, the team used a RF classification with a maximum of 2000 trees and a maximum tree depth of 50. The team selected to use a maximum of 2000 samples per class with the following segment attributes: active chromaticity color, mean digital number, and standard deviation. In the Classify window, the team ran the model to create classified images for both years.

The classification of the NAIP imagery was conducted in GEE using a pixel-based RF script from the NASA DEVELOP Code Examples GEE repository, created by the Colorado State University Natural Resource Ecology Lab. The script compiled ancillary data and composited them into a single image. Because of the fine resolution of the pixels and the large size of the images, the classification was run on the county level instead of the whole state. In addition, a fifth class for Forest/Cropland was added, as the high resolution of the NAIP imagery provided better differentiation between vegetative signatures. The script produced an overall training accuracy assessment and a confusion matrix, an array where one axis showed the true values of a selection of training points, and the other predicted values derived from the classifier methodology. An r^2 score was also calculated as a measure of overall accuracy.

To perform land cover change analysis and produce forecasted maps, the team used LCM tool in TerrSet. Raster files of the classified Landsat satellite images were converted from .tif to .rst format using the Geospatial Data Abstraction Library (GDAL) Conversion Utility. Next, the team mapped transitions from 2010

to 2020 for each of the four classes. After mapping change over the past decade, the team created groups of class transitions, theorized to be reactive to similar drivers of change. These groups were chosen to most accurately reflect wetland dynamics that are likely to impact future loss or gain. For wetland loss predictions, the team used a sub-model that included transition from Wetland to Developed, Non-wetland Vegetation, and Water. For wetland gain predictions, a model was chosen that included transition from Non-Wetland Vegetation to Wetland; the transition from developed land to wetland was excluded due to low likelihood, and water to wetland was excluded due to the small area of change for the current study period, and confusion in modeling the similar spectral signature of the two classes. The team chose to run loss and gain models separately, as well as in conjunction, because of LCM limitations at modeling different drivers of change.

To increase the real-world accuracy of the model, the team added raster images of roads and elevation as static layers. After bringing in all relevant data, the team ran a Multi-Layer Perceptron (MLP) neural network to analyze each model. The tool calculated changes and persistence in pixels between the two initial study years for each given model, then ran 10,000 iterations of predictive training to determine the model's skill at predicting the transition of each pixel. After receiving information about the model's accuracy, LCM created Transition Potential maps for each possible class transition, which indicated the potential for class transition across the study area. Next, LCM created a Markov Chain prediction, indicating the likelihood of transition between all classes. The team created soft and hard predictions of land cover for the chosen prediction year. Soft predictions indicated the potential of land cover transformation by the prediction year, while the hard prediction demonstrated a commitment to a single scenario of change. A layer of Delaware Public Protected Lands from 2019, accessed from FirstMap, was used as a mask to indicate areas of protection from change. This enabled the team to examine the significance of maintaining protected wetland areas. The models were also run without using the protected public lands layer. The team created predictions for every five years, from 2025 to 2050, for each model.

3.3.2 Tidal Marsh Suitability

Suitable locations for marsh migration based on impervious surfaces, hydric soils, slope, water availability, and agricultural land were analyzed in ArcGIS Pro using the Suitability Modeler. The model used a suitability score from one to five (one being the least suitable and five being the most suitable) with specific weights given to each criterion. The reclassified impervious surfaces layer was added to the Suitability Modeler under Unique Values and Field selection was set to Value. The developed areas were given a suitability score of 1 while the undeveloped areas were given a score of 5.

After adding the soils data to the modeler, the team chose the Unique Categories option for this dataset in order to rank each drain class from one to five, five being the most suitable. Soil drainage class described the frequency and duration of soil saturation due to high water tables. The most ideal drainage classes for wetland formation and persistence were very poorly drained, poorly drained, and somewhat

poorly drained. The drain classes were ranked as follows: 5 – Very poorly drained, 5 – Poorly drained, 4 – Somewhat poorly drained, 3 – Moderately well-drained, 2 – Well drained, 2 – Somewhat excessively drained, 1 – Excessively drained, 1- Subaqueous, 1 – No Data.

The team added the resampled slope layer into the Suitability Modeler under Continuous Functions. The function was set to MSSmall, used when small criterion values have a much higher preference, because of a preference for small slope values for marsh migration. The cropland data was added to the Suitability Modeler under Unique Values. Land with crops present was given a suitability score of 1, while land free of crops was given a score of 5. The flowlines data layer was added to the Suitability Modeler under Continuous Functions. Because low distances from flowlines are preferred, the function was also set to MSSmall. Land that is closer to rivers or streams was considered more suitable for marsh migration. However, this close proximity to flowlines does not explicitly indicate tidal influence. After each layer went through its respective transformations, the team ran the suitability model at full resolution. The Locate tool was used to identify the top five most suitable locations based on the highest average suitability score. Using the Locate Regions tool or Locate tab within the Suitability Modeler, the team used a shapefile of current tidal marsh locations to identify areas that do not fall within current tidal marshland. We ran several iterations of the Locate tool to identify areas of land that currently contain freshwater wetlands and are also adjacent to tidal wetlands.

3.3.3 Climate Analysis

In QGIS, an average for the years 2000-2015 was created using the Calculate Raster tool. The same tool was used to calculate the difference in seasonal precipitation and temperature between the 2000 to 2015 average and the 2015 to 2020 average. The seasonal maps that were created from this provided the team with seasonal precipitation and temperature difference maps that allowed the team to see variation in these variables between the two average periods.

The exported CSV data file from GEE was imported into Microsoft Excel to perform the monthly and seasonal trend analyses. To perform seasonal trend analysis, the team categorized monthly averages for temperature and precipitation data of each year into each of the four seasons. The seasonal measurements were then plotted using a scatterplot graph resulting in 8 individual graphs (two for each season: precipitation and temperature). The monthly data was plotted in a single scatterplot graph for each metric. A Power Regression Trendline was calculated for both analyses and added to each graph to visualize a general, linear trend of patterns for the study interval. This trendline was also projected out to 2025 for all graphs.

4. Results & Discussion

4.1 Analysis of Results

4.1.1 Land Use Land Cover Change

In total, RF classification was run five times to create five different images (2010 Landsat 5 TM image, 2020 Landsat 8 OLI image, 2018 NAIP image for New Castle County, 2018 NAIP image for Kent County, and 2018 NAIP image for Sussex

County). The Image Classification Wizard calculated an overall r^2 accuracy score for the two Landsat images, while the GEE script did the same for the three NAIP images. An r^2 score (also known as a coefficient of determination) is a statistical measure of accuracy that describes how well variation within a dependent variable is explained by the independent variable. A higher r^2 score indicates that they are more similar, while a lower r^2 indicates that they are less similar. In this case, the r^2 score indicates the proportion of the training data that would be properly classified if run through the RF process (Table 5).

Table 5
Classified images created and their respective r^2 values

Image	**r^2 Value**
2010 Landsat 5	0.9567
2020 Landsat 8	0.9681
2018 NAIP New Castle County	0.9136
2018 NAIP Kent County	0.8826
2018 NAIP Sussex County	0.8758

The results of the RF classification were then loaded into the LCM. During change analysis, in which changes over the study period were assessed, LCM found that there was both gain and loss in wetland area during the study period. The results of the change analysis can be seen in Table 6. The majority of wetland pixels persisted through the time period, while the smallest class of pixels were those who transitioned into wetland from other classes. Accounting for all loss and gain, there was a net loss of 4,434.05 acres of wetland area between 2010 and 2020.

Table 6
The area of wetland gain, loss, and persistence during the study period from 2010 to 2020.

Wetland Change (2010-2020)	**Area (Acres)**
Loss	57,829.91
Gain	53,395.86
Persistence	116,268.87

As part of the learning process to create Transition Potential maps, LCM produced a report for each grouped sub-model of class transitions to indicate the success at predicting pixel changes for each class between the 2010 and 2020 images. This helped the team determine which class transitions to group together for the predictive sub-models, and provided feedback about which variables had the greatest effect on model skill. Table A1 in Appendix A presents accuracy and skill assessments for the two final models of change based on current patterns of wetland loss and gain. Unfortunately, due to the limitations of LCM at modeling the effects of different drivers of change, the maps produced are limited in their capacity to accurately reflect future land cover change. As noted in the methodology, the first model followed patterns of wetland loss transitions from wetland to water, developed land, and non-wetland vegetation. The second model followed patterns of wetland gain transitions from non-wetland vegetation to wetland. A third model, following the loss and gain patterns of the first two models, was created as well.

By following these different models of prediction, the team was able to create maps that demonstrate possible land cover outcomes for every five years out to the year 2050. LCM produced both soft and hard predictions for each year, with the soft prediction representing the potential for class transition, and the hard prediction demonstrating one possible scenario for land cover. Figure 2 shows a hard prediction of 2050 land cover from a model following current wetland loss patterns, with the addition of a mask of public protected lands. This model predicted a total loss of 105,939.13 acres of wetland by 2050 (Table A2). Figure 3, on the other hand, shows the results of a model that followed current patterns of wetland gain, specifically from wetland to non-wetland vegetation. The team also included the mask of public protected lands as part of the wetland gain predictions. This model predicted wetland gain amounting to 49,256.39 acres by 2050 (Table A3). The model that incorporated both loss and gain indicated a predicted net loss of wetland area amounting to 56,559.67 acres by 2050, given current public protected lands (Table A4, Figure A1), compared to 2050 net loss of 56,570.16 acres in the model without protected lands (Table A5, Figure B2). Soft predictions of the models are located in Appendix A (Figures A5 – A7).

4.1.2 Tidal

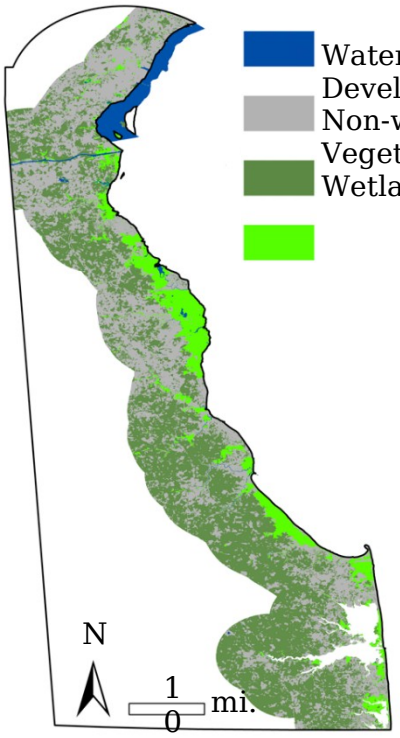

Figure 2 Predicted 2050 land cover, based on current patterns of wetland loss and a mask of public protected lands.

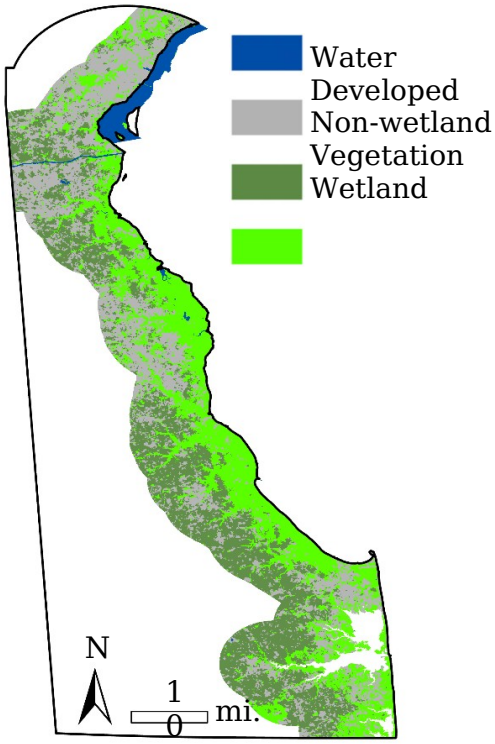

Figure 3 Predicted 2050 land cover, from wetland gain model based on current patterns of transition from wetland to non-wetland vegetation.

Marsh Suitability

After several iterations of the suitability model which involved altering the weight assigned to each criterion, a final suitability map was created. Red, yellow, and green portions of the map describe areas least suitable, moderately suitable, and most suitable, respectively (Figure 4). Based on the results of the Locate Regions tool, many of the most suitable areas were in the southern part of the state. However, most of these areas were too far from the coast and were not close to existing saltwater tidal marshes. Since the partners were interested in areas that have the potential to shift from freshwater marsh to saltwater marsh, these areas

were not included in the final product. The top five most suitable plots of land were located in the middle of the Delaware coastline located in Kent County (See Figures B1-B3).

The suitability map can be used in combination with the LULC projection maps to identify land parcels where conservation efforts would be most successful. Figures B4 and B5 in Appendix C show the LULC change results for wetland loss and gain in the year 2050 overlaid with the top five most suitable locations for marsh migration within the coastal zone. Together these overlaid layers indicate which suitable locations may have the greatest long-term success for restoration or preservation projects, given current patterns of wetland change. For instance, in the wetland loss scenario, location four falls adjacent to an area predicted to persist as wetland by 2050, and may offer greater success as an area for wetland preservation than other locations that fall well outside the predicted 2050 wetland area.

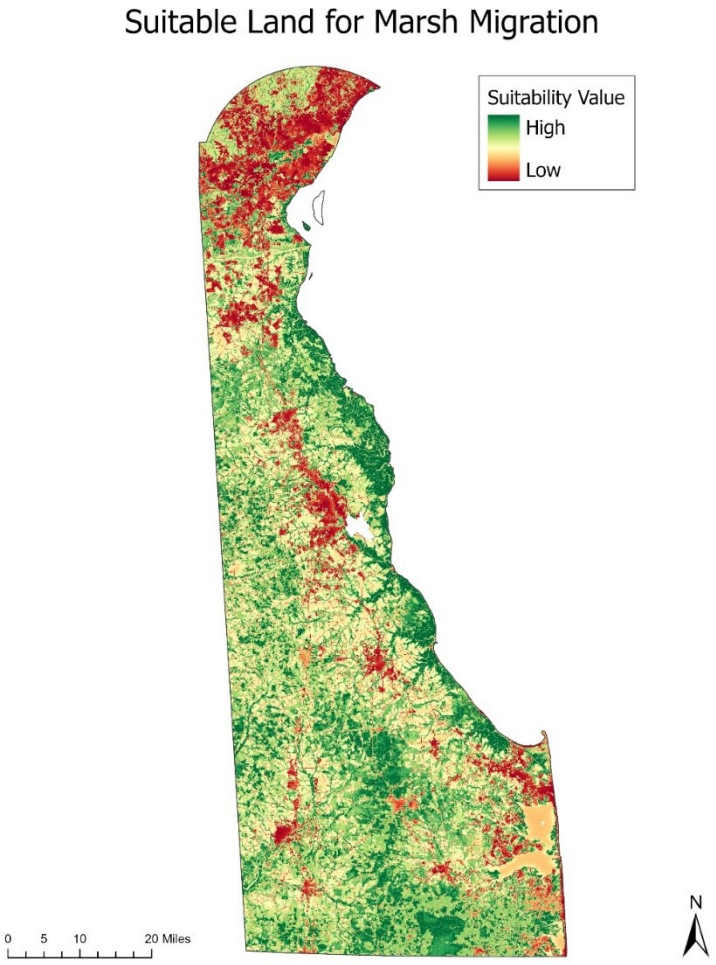

Figure 4. Marsh migration suitability map created for the state of Delaware based on five environmental variables.

4.1.3 Climate Analysis

After creating maps depicting the difference between temperature and precipitation averages from 2000 to 2015 and 2015 to 2020, conclusions from the maps and data were drawn. Starting with precipitation (Figure C1), it is seen that summer has the largest increase in seasonal precipitation, while fall has the largest decrease. These maximum and minimum differences occur in the northern portion of the state. This is likely because of its proximity to hills and slope variation. Looking at temperature (Figure 6), the largest increase in seasonal temperature occurs in winter. Fall also sees an increase while spring and summer sees slight decrease. These observations can be important in analyzing marsh migration and wetland formation or destruction because they provide possible reasoning for loss or gain. It is important to note that climate variability is more accurate and definitive when a longer time period is used. Due to the constraints of this project, only a 20-year time period was able to be analyzed.

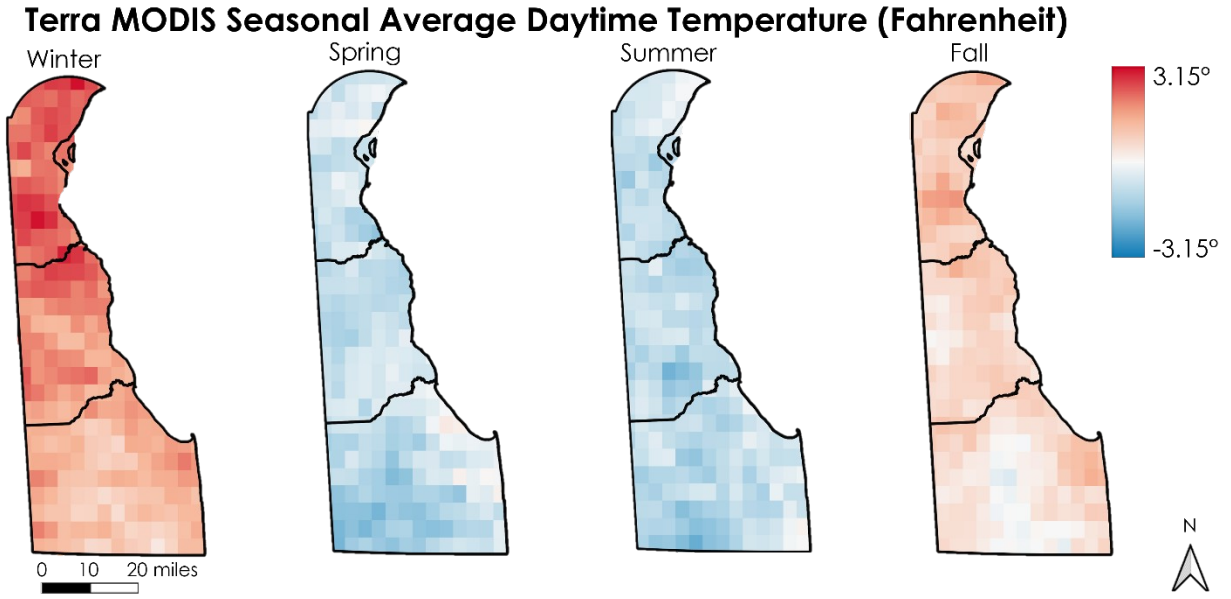

Figure 5. Difference maps of average seasonal daytime temperature change from 2000-2015 to 2015-2020.

Seasonal trends in Delaware remain relatively consistent over the last 20 years. This could be related to the proximity to the Atlantic Ocean which aids in stabilizing annual temperatures and precipitation. Temperature fluctuation in spring (Figure C2) and fall (Figure C3) have the greatest difference between the maximum and minimum temperatures through the season while summer months have a linear, stable temperature pattern (Figure C4). Winter, however, shows a sharper incline in linear trend than the other seasons (Figure C5) and seems to have a steady increase in temperature since 2000. Precipitation patterns in spring (Figure C6) and summer (Figure C7), though scattered, show a relatively flat trendline indicating no significant increase or decrease over the time period. Winter (Figure C8) and fall (Figure C9) precipitation patterns demonstrate an increasing trend since 2000. Though this is the case, winter months show the highest increasing trend overall for the last 20 years. This trend can be seen in the northern region of Delaware (Figure 5) which could be a result of urbanization and slope variation in the area. Overall, there is a general increasing trend among the

climate variable across Delaware (Figure C10 and C11). As a note, linear regressions do not provide high accuracy assessments for non-linear data such as the data used in this study. The graphs produced for this section (Appendix C) are to be used as informative guides for climatic trends in Delaware and are subject to change.

4.2 Future Work

Due to the complexities of tidal marsh systems and the factors that impact them, there are several variables affecting marsh migration potential that were not able to be analyzed in this short-term study. Variables identified by both the DEVELOP team and DNREC include the effects of land subsidence, marsh drowning, wind fetch, and edge erosion on the formation of tidal marsh habitat. In addition, future work on this topic could include analyzing regression relationships between different variables and tidal marsh suitability to aid in the creation of a repeatable model that would predict tidal marsh suitability in specific areas of interest. Future areas of research could focus on implications of different sea-level rise scenarios, regionally specific LULC studies to include more classes, endangered species affected by coastal marsh habitat loss, and ways to implement conservation methods, as well as detailed salinity studies to identify and analyze different types of tidal marsh systems. Moving forward, our team would suggest choosing a smaller area of interest due to time constraints, processing obstacles, and the possibility of a more detailed analysis of tidal marsh processes.

5. Conclusions

While there was observed wetland loss in many parts of Delaware between 2010 and 2020, there was a substantial amount of gain (57,829.91 acres of loss versus 53,395.86 acres of gain). The results show that while significant wetland loss (wetland becoming non-wetland vegetation, developed, and water) is a likely outcome for many wetland areas, there are areas where transitions from non-wetland vegetation to wetland is likely. Sea-level rise may result in some coastal wetland loss, it may also contribute to wetland gain further inland, particularly in vegetated areas with low elevation. Seasonal trends in Delaware's climate remained relatively consistent over the last 20 years. Of all the seasonal trends, winter had the highest increasing pattern over the time interval of this study in both precipitation and temperature measurements.

Suitable land for marsh migration and conservation based on five environmental factors were identified through suitability analyses. Though much of the suitable land is currently covered by tidal marsh, suitable non-wetland land was identified throughout the state with the most suitable land parcels located in Kent County. The LULC change maps can be used in combination with the suitability maps to gain a better perspective on which sections of land would be most feasible for conservation success in the future.

6. Acknowledgments

The team would like to thank our science advisors, Dr. Jeffrey Luvall at NASA Marshall Space Flight Center, Dr. Robert Griffin at the University of Alabama in Huntsville, and our NASA DEVELOP Fellow A. R. Williams for their insight and guidance on the project end products. Also, the project partners at DNREC whose knowledge and excitement about the project drove the team to produce the best end products possible.

Any opinions, findings, and conclusions or recommendations expressed in this material are those of the author(s) and do not necessarily reflect the views of the National Aeronautics and Space Administration.

This material is based upon work supported by NASA through contract NNL16AA05C.

7. Glossary

DNREC – Delaware Department of Natural Resources and Environmental Control
Earth observations – Satellites and sensors that collect information about the Earth's physical, chemical, and biological systems over space and time
GPM – Global Precipitation Measurement Core Observatory
Land Change Modeler (LCM) – A tool within TerrSet that is adept at quantifying land change between two dates, creating transition potentials for specific classes, and predicting land change into the future
MODIS – Moderate Resolution Imaging Spectroradiometer
NAIP – National Agriculture Imagery Program
Power Regression Trendline – A curved line used on datasets that compare measurements that change
over a specific rate (months/years)
Random Forest (RF) Algorithm – a type of machine learning algorithm designed for classification or regression. In classification, random forest runs several decision tree algorithms that categorically 'vote' on how individual pixels should be classified
Sudden Wetland Dieback – A condition characterized by the rapid, partial, or complete death of emergent saltmarsh vegetation

8. References

Barbier, E. B., Hacker, S. D., Kennedy, C., Koch, E. W., Stier, A. C., & Silliman, B. R. (2011). The Value of Estuarine and Coastal Ecosystem Services. (A. M. Ellison, Ed.) *Ecological Monographs*, *81*(2), 169- 193. Retrieved from https://doi.org/10.1890/10-1510.1

Blankespoor, B., Dasgupta, S., & Laplante, B. (2014). Sea-Level Rise and Coastal Wetlands. *AMBIO 43*(8),996-1005. doi:https://doi.org/10.1007/s13280-014-0500-4

Correll, M. D., Hantson, W., Hodgman, T. P., Cline, B. B., Elphick, C. S., Gregory Shriver, Tymkiw, W.& Olsen, B. J. (2018). Fine-Scale Mapping of Coastal Plant Communities in the Northeastern USA. *Wetlands 39*: 17-28. https://doi.org/10.1007/s13157-018-1028-3

DNREC. (n,d,). *Topic: Wetlands*. DNREC Alpha. https://dnrec.alpha.delaware.gov/wetlands/.

Lamb, B. T., Tzortziou, M. A., & McDonald, K. C. (2019). Evaluation of Approaches for Mapping Tidal Wetlands of the Chesapeake and Delaware Bays. *Remote*

Sensing, *11*(20), 2366. MDPI AG. Retrieved from http://dx.doi.org/10.3390/rs11202366

Rogerson, A., A. Howard, & A. Jacobs (2009). Wetlands condition of the Inland Bays watershed. Volume 2. Delaware Department of Natural Resources and Environmental Control, Watershed Assessment Section, Dover, Delaware USA.

Tiner, R. W., Biddle, M. A., Jacobs, A. D., Rogerson, A. B., & McGuckin, K. G. (2011). *Delaware Wetlands: Status and Changes from 1992 to 2007* (p. 35) Cooperative National Wetlands Inventory Publication. U.S. Fish and Wildlife Service and the Delaware Department of Natural Resources and Environmental Control. https://documents.dnrec.delaware.gov/Admin/DelawareWetlands/Documents/Delaware%20Wetla nds%20Status%20and%20Changes%20from%201992%20to%202007%20FINAL2012.pdf

Wang, X., Gao, X., Zhang, Y., Fei, X., Chen, Z., Wang, J., Zhang, Y., Lu, X., & Zhao, H. (2019). Land-Cover Classification of Coastal Wetlands Using the RF Algorithm for Worldview-2 and Landsat 8 Images. *Remote Sensing*, *11*(16), 1927. https://doi.org/10.3390/rs11161927

9. Appendices

Table A1
Assessments of LCM predictive accuracy rate and skill measure for sub-models that measure wetland loss and gain, as established from 2010 and 2020 class transitions. Accuracy rate refers to the model's ability to predict whether validation pixels would change. Skill measure was calculated by subtracting accuracy expected by chance from the measured accuracy.

Transitions Included in Sub-Model	**Accuracy Rate**	**Skill Measure**
Wetland Loss: Wetland to Water, Developed, and Non-Wetland Vegetation	57.75%	0.4367
Wetland Gain: Non-Wetland Vegetation to Wetland	66.30%	0.3259

Table A2
Transitions from wetland to other classes by 2050, in a predictive model of wetland loss with a mask of public protected lands from 2019.

Type of Transition	**Area of Wetland Loss by 2050 (Acres)**	**Total Wetland Loss by 2050 (Acres)**
Wetland to Water	1,541.14	105,939.13
Wetland to Developed	51,798.48	
Wetland to Vegetation	52,599.51	

Table A3
Transitions from other classes to wetland by 2050, in a predictive model of wetland gain that includes current patterns of change from non-wetland vegetation to wetland. Prediction included a mask of public protected lands from 2019.

Type of Transition	**Area of Wetland Gain by 2050 (Acres)**
Vegetation to Wetland/Total Gain	49,256.39

Table A4
Changes in wetland area by 2050, as determined by a predictive model of wetland loss and gain with the inclusion of a public protected lands mask. Corresponds to Figure A1.

Type of Transition (2050)	**Area (Acres)**	**Total Wetland Loss or Gain (Acres)**	**Net Total Wetland Loss (Acres)**
Non-Wetland Vegetation to Wetland	49,302.11	49,302.11	56,559.67
Wetland to Water	1,541.14	105,861.78	

Wetland to Developed	51,849.48		
Wetland to Non-Wetland Vegetation	52,471.16		

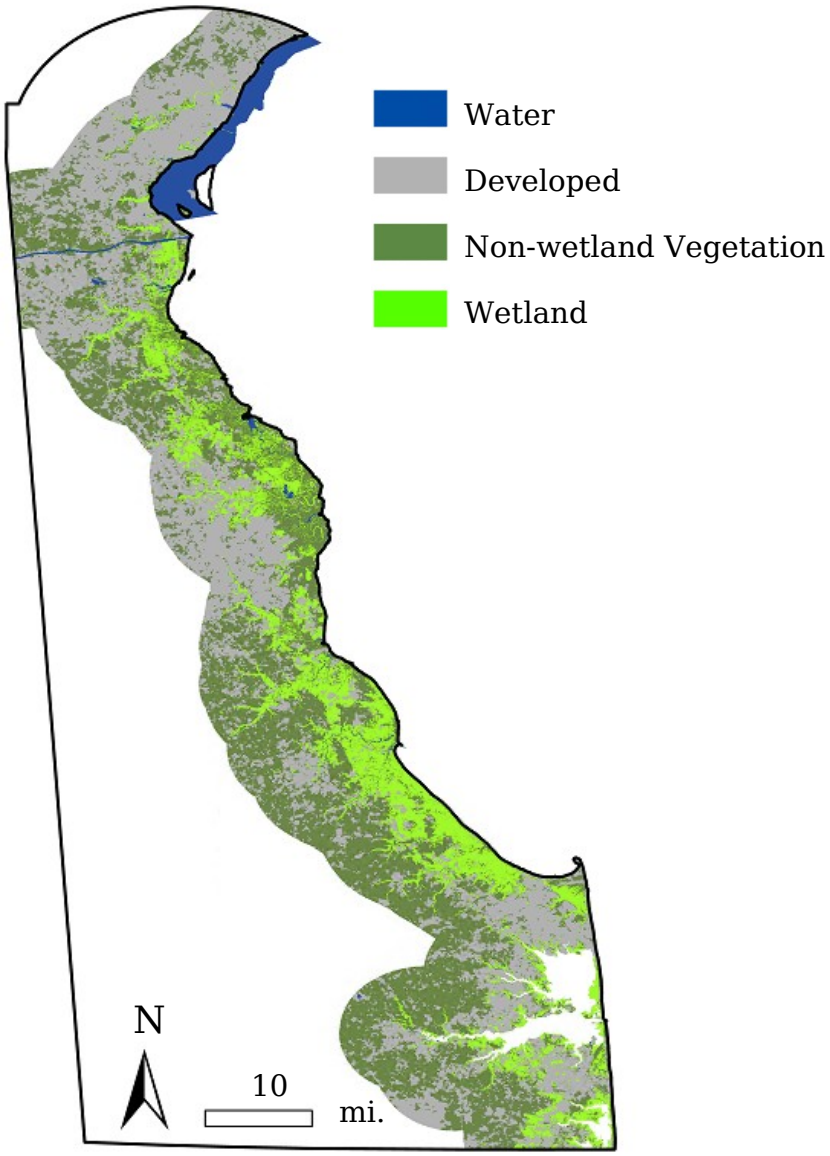

Figure A1. Predicted 2050 land cover, based on a model that included current patterns of both loss and gain. This prediction included a mask of public protected lands as an incentive.

Table A5

Changes in wetland area by 2050, as determined by a predictive model of wetland loss and gain without a public protected lands mask. Corresponds to Figure A2.

Type of Transition (2050)	**Area (Acres)**	**Total Wetland Loss or Gain (Acres)**	**Net Total Wetland Loss (Acres)**
Non-Wetland Vegetation to Wetland	49,294.33	49,294.33	56,570.16
Wetland to Water	1,542.26	105,864.49	
Wetland to Developed	51,719.32		
Wetland to Non-Wetland Vegetation	52,602.91		

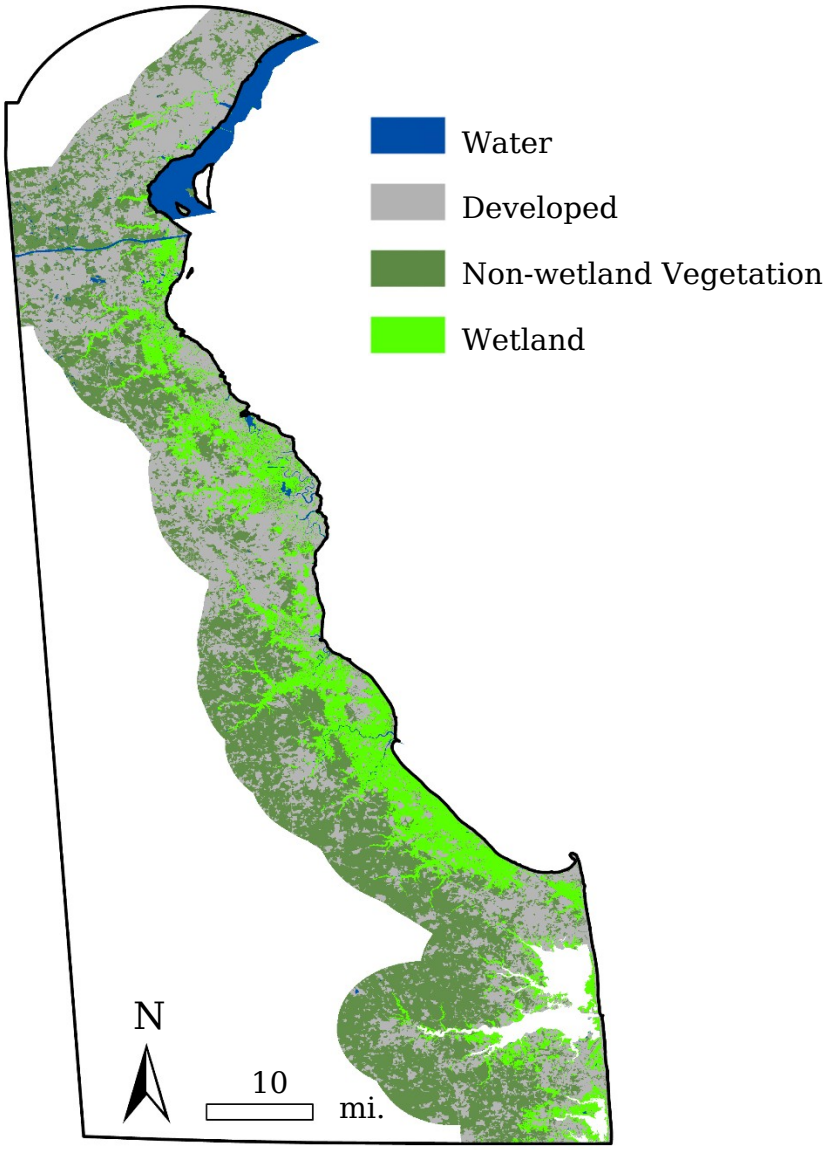

Figure A2. Predicted 2050 land cover, based on a model that included current patterns of both loss and gain. This prediction did not use a mask of public protected lands, resulting in slight differences in predictions made by the model that incentivized areas of protected land, and overall, slightly greater net wetland loss.

Table A6
Transitions from wetland to other classes by 2050, as predicted by a model of wetland loss without a public protected lands mask. Corresponds to Figure A3.

Type of Transition (2050)	**Area of Wetland Loss (Acres)**	**Total Loss (Acres)**
Wetland to Water	1,542.26	

Wetland to Developed	51,749.41	105,864.43
Wetland to Vegetation	52,572.76	

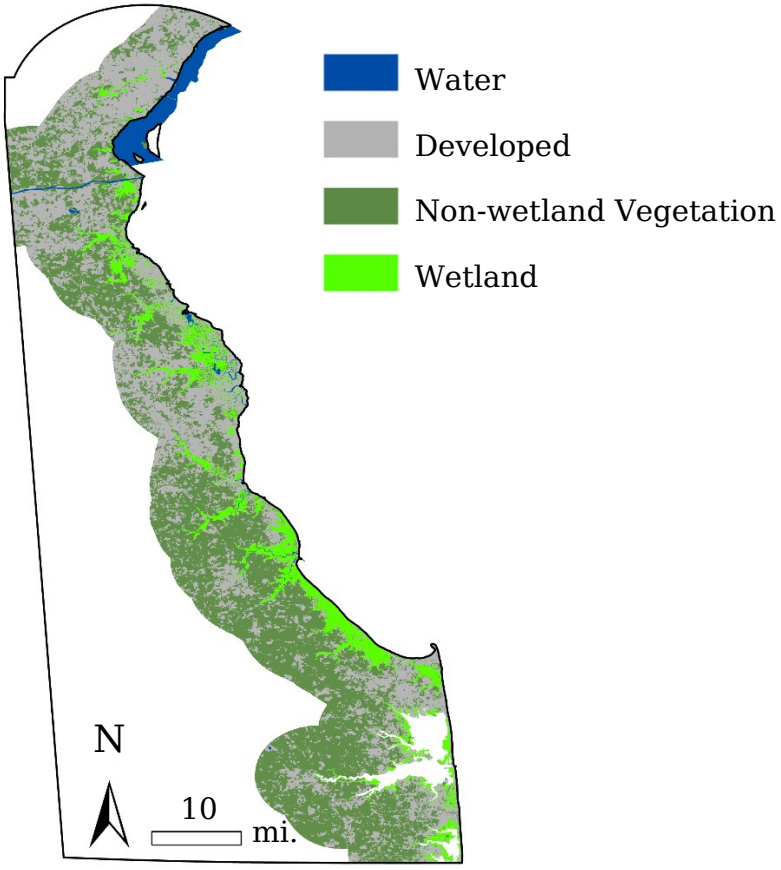

Figure A3. Predicted 2050 land cover, based on a wetland loss model created from current patterns of wetland loss transitions from wetland to developed, non-wetland vegetation, and water. This prediction did not use a mask of public protected lands as an incentive, resulting in some predicted transition from wetland to developed area in places that were classified as protected lands in 2019, such as the area in and around Bombay Hook National Wildlife Refuge.

Table A7
Transitions from non-wetland vegetation to wetland by 2050, as determined by a predictive model of wetland gain without a public protected lands mask. Corresponds to Figure A4.

Type of Transition (2050)	**Area of Wetland Gain (Acres)**
Non-Wetland Vegetation to Wetland/Total Gain	49,294.18

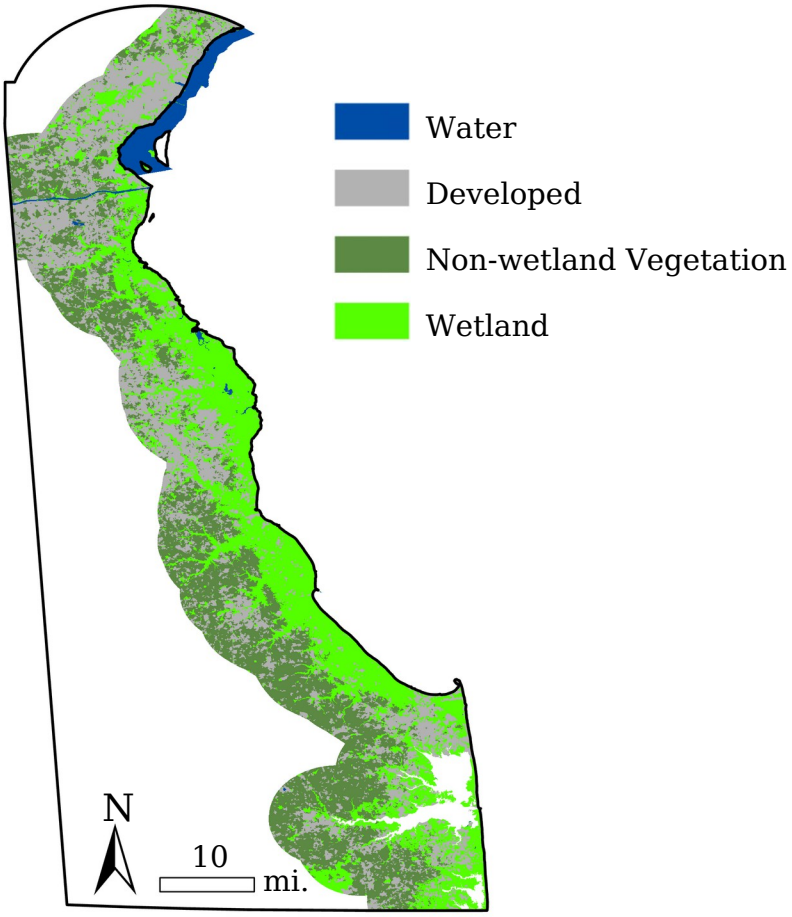

Figure A4. Predicted 2050 land cover, based on a wetland gain model created from current patterns of transition from non-wetland vegetation to wetland. This prediction did not use a mask of public protected lands as an incentive, resulting in slight differences in predictions made by the model that incentivized areas of protected land.

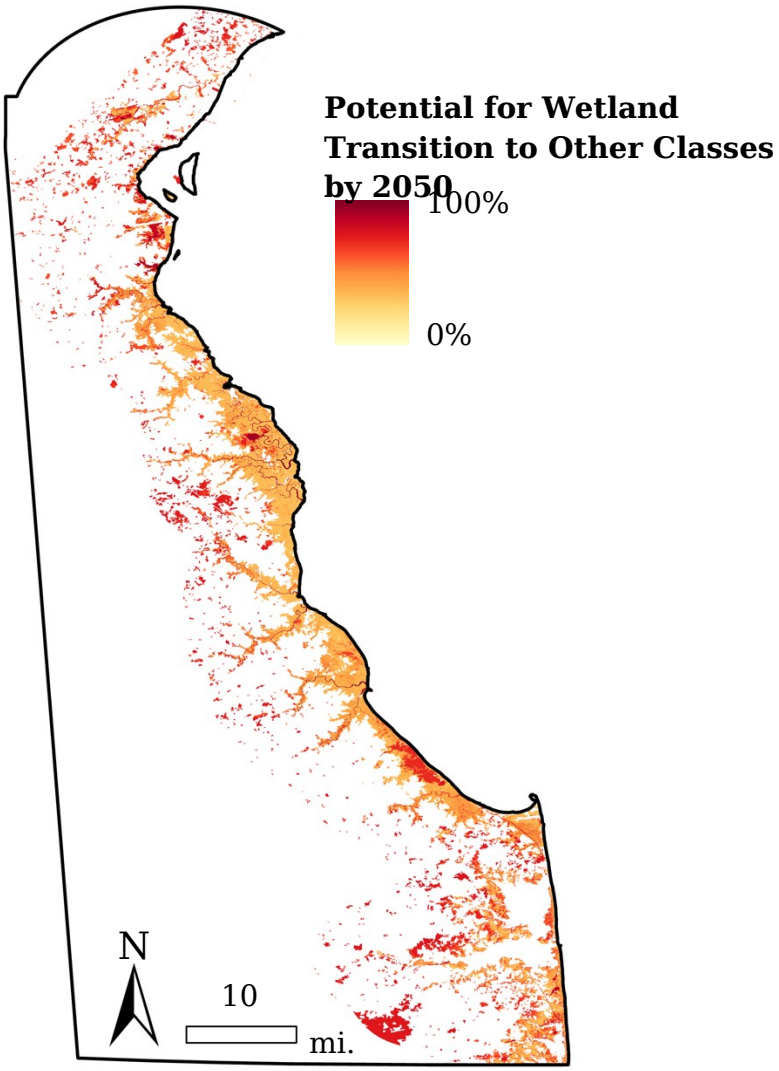

Figure A5. Soft prediction of land cover change by 2050, as determined by a model of wetland loss created from current patterns of transition from wetland to water, developed land, and non-wetland vegetation. Layers of elevation and roads in the study area were included in determining wetland loss potential.

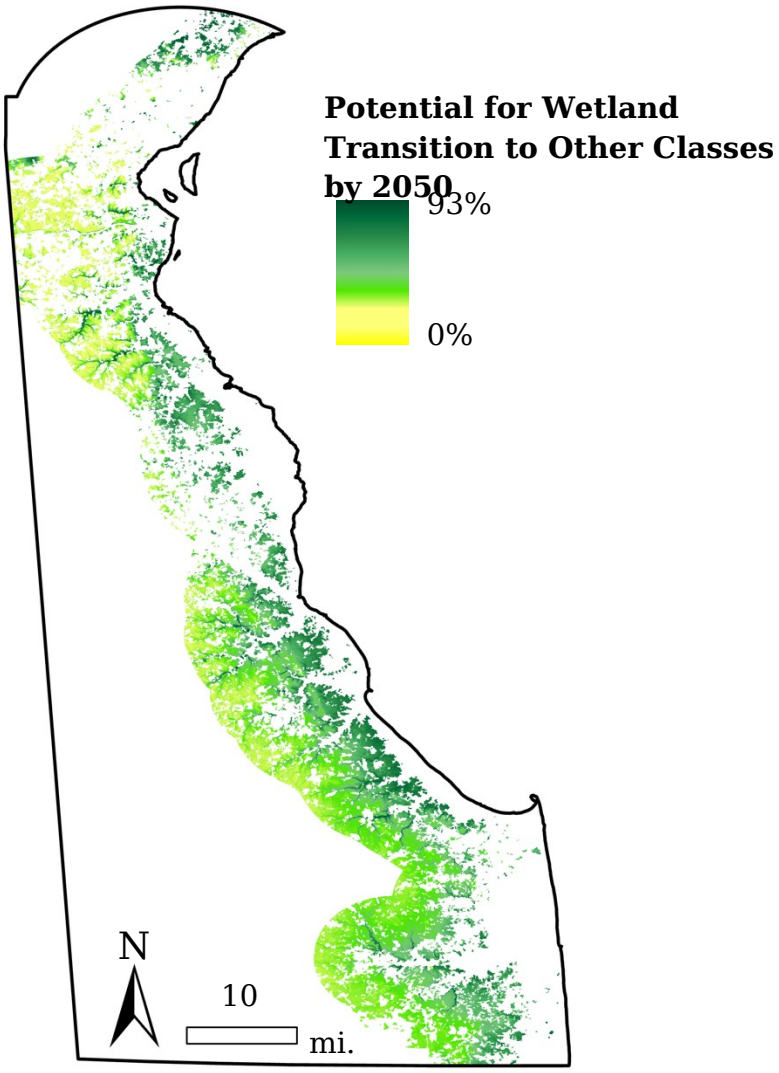

Figure A6. Soft prediction of land cover change by 2050, as determined by a model of wetland gain created from current patterns of transition from non-wetland vegetation to wetland. Layers of elevation and roads in the study area were included in the determination of wetland gain potential, and the likelihood of inland wetland gain is higher in areas with low elevation.

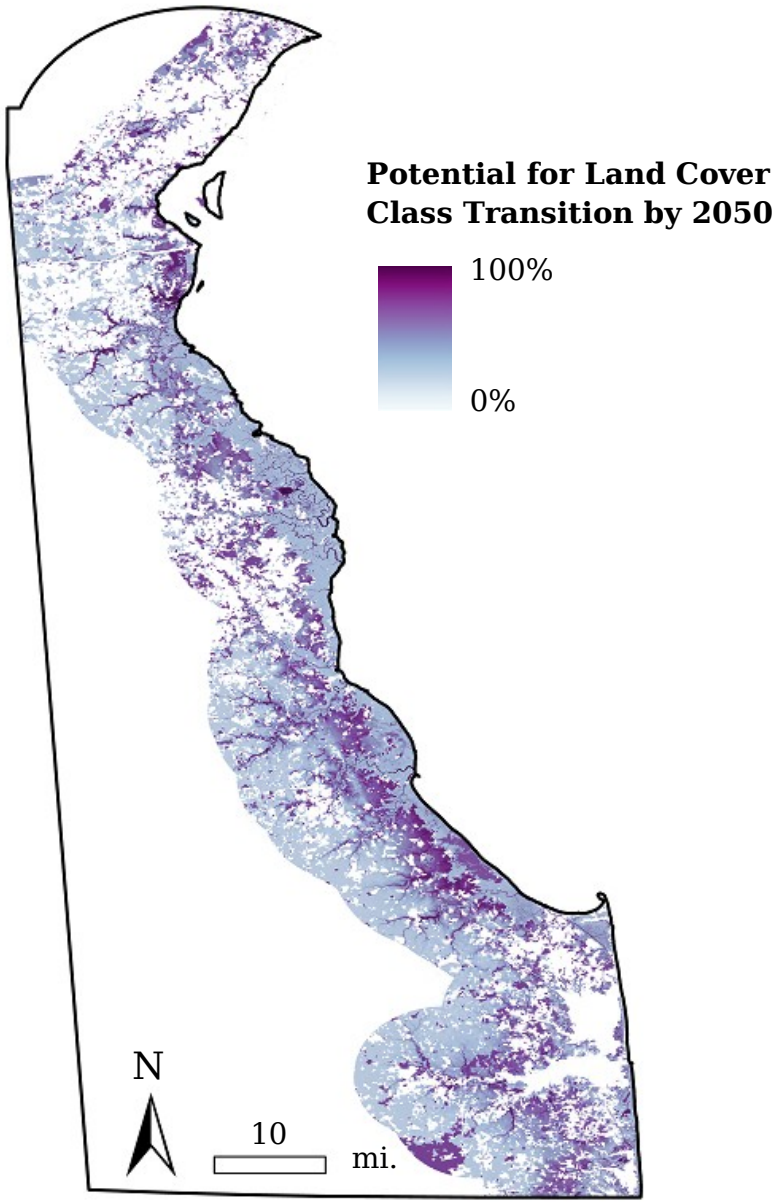

Figure A7. Soft prediction of land cover change by 2050, as determined by a model of combined wetland gain and loss. Layers of elevation and roads in the study area were included in the determination of change potential. This map indicates not only wetland change potential, but vulnerability to change across all four land cover classes used in the model.

Appendix B – Tidal Marsh Suitability

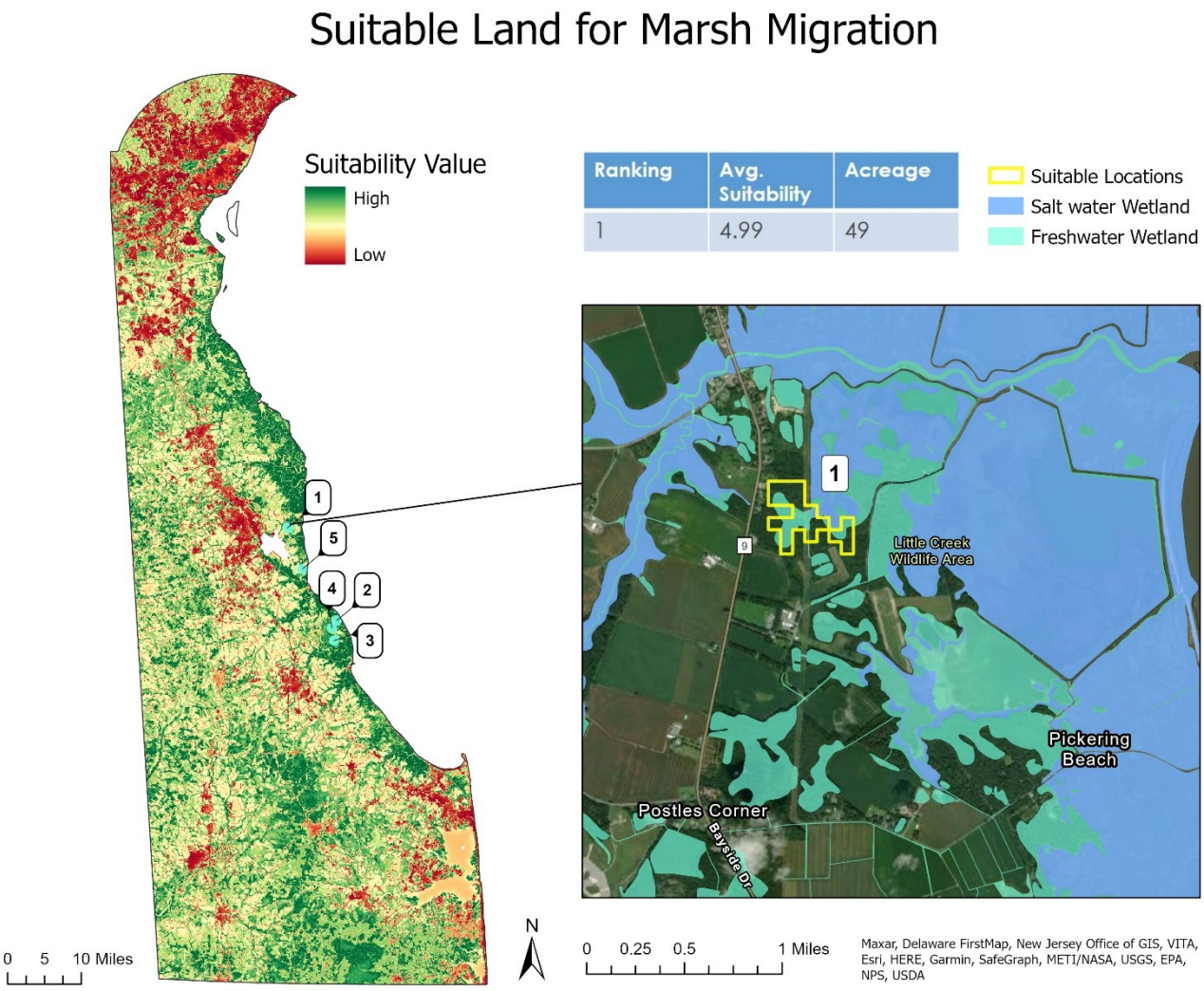

Figure B1. A suitability map identifying suitable land containing freshwater wetlands that are also adjacent to tidal wetlands. This map shows the plot of land with the highest suitability rating located near the Little Creek Wildlife Area and Pickering Beach.

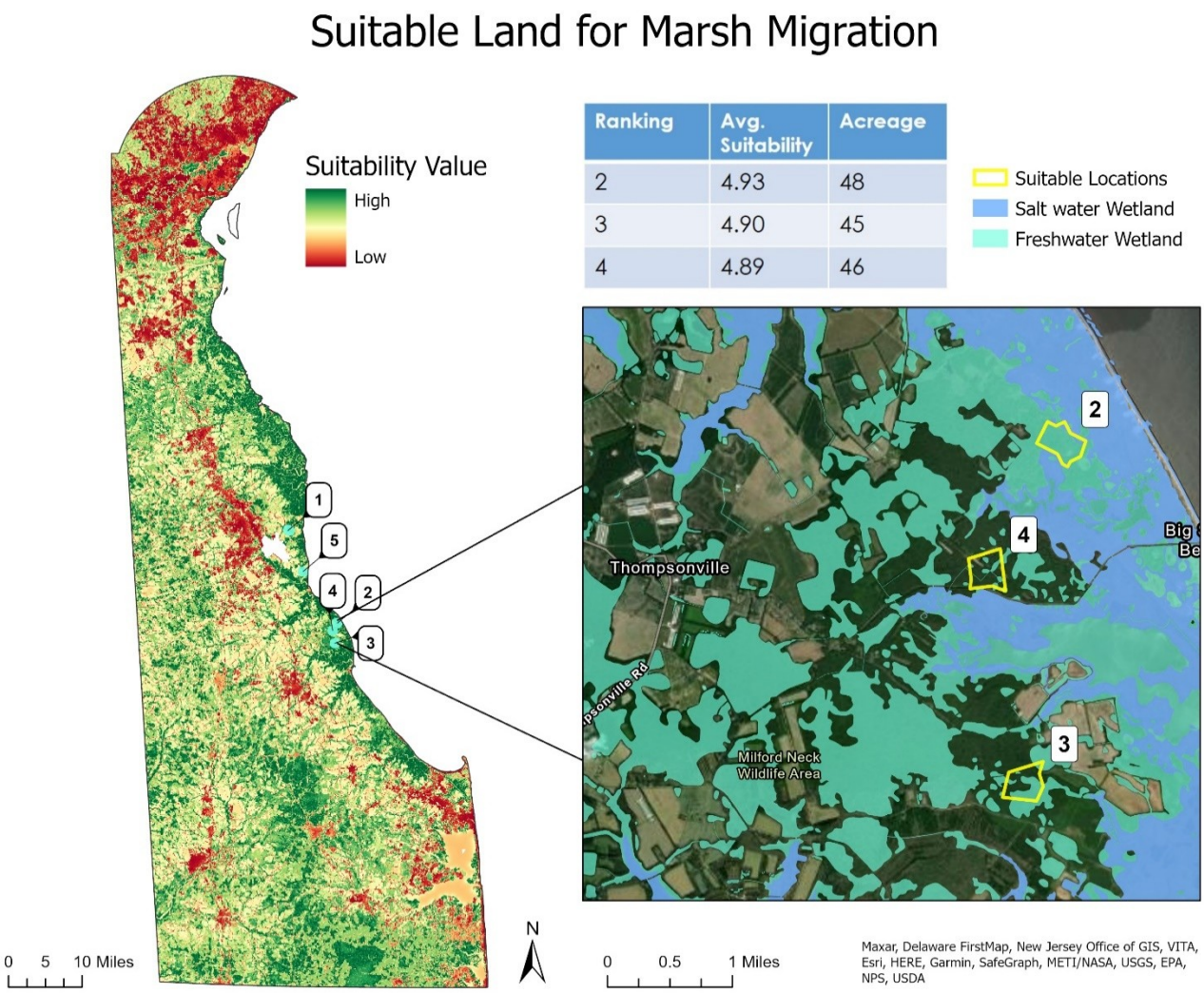

Figure B2. A suitability map identifying suitable land containing freshwater wetlands that are also adjacent to tidal wetlands. This map shows land ranked 2-4 located near Big Stone Beach and the city of Thompsonville.

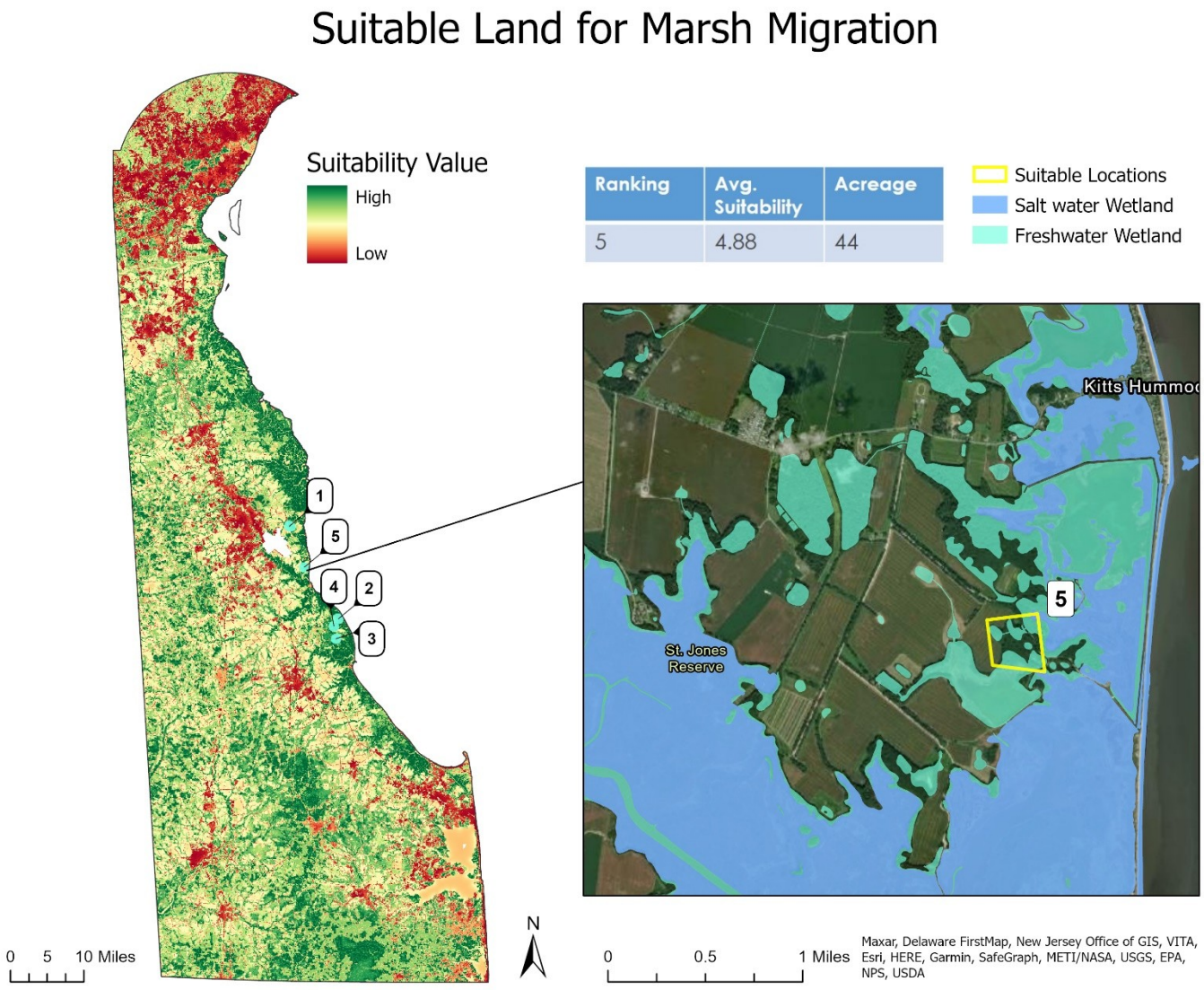

Figure B3. A suitability map identifying suitable land containing freshwater wetlands that are also adjacent to tidal wetlands. This map shows the 5th most suitable area of land located near St. Jones Reserve and the community of Kitts Hummock.

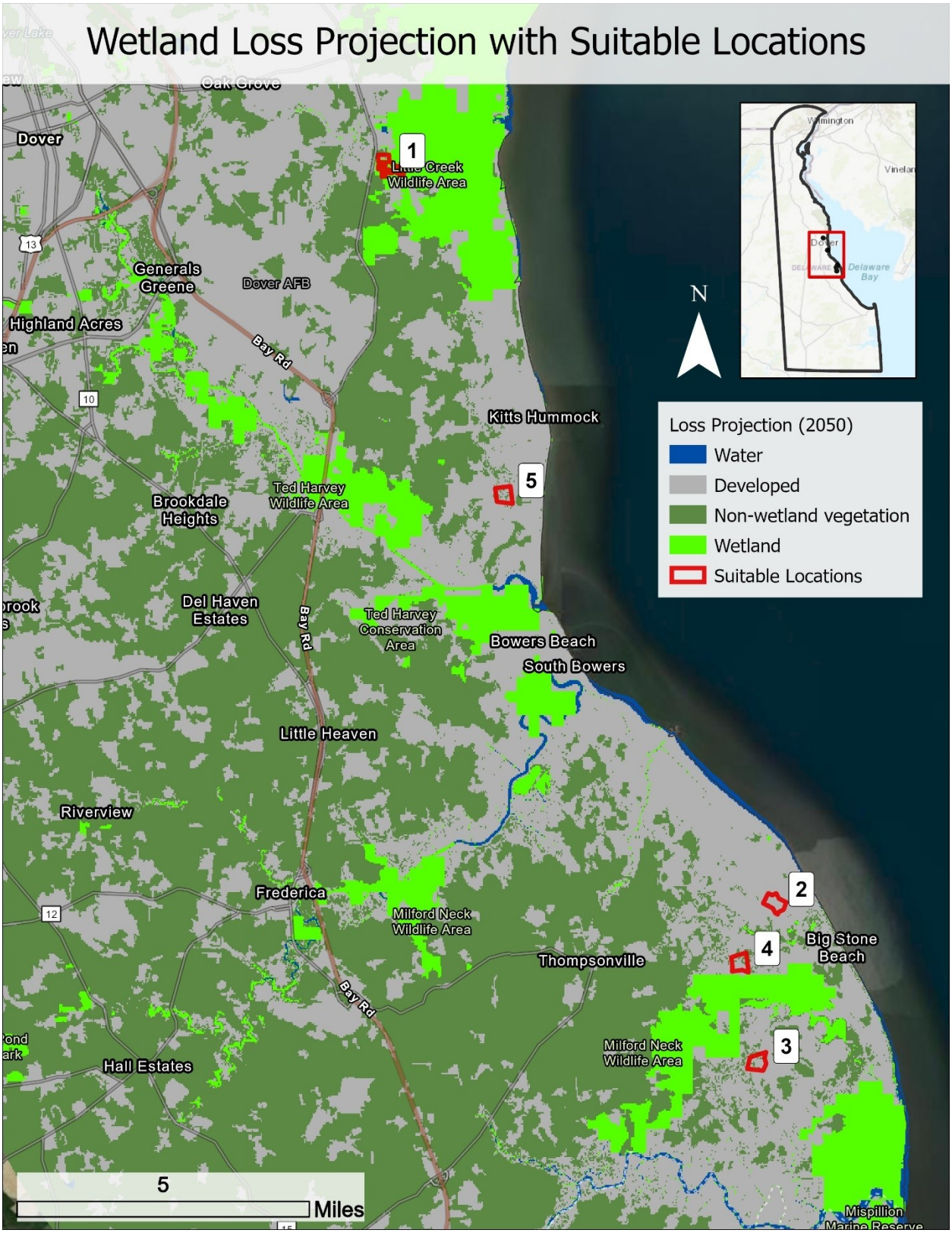

Figure B4. Top five suitable locations for marsh migration overlaid with the LULC change 2050 wetland loss projection.

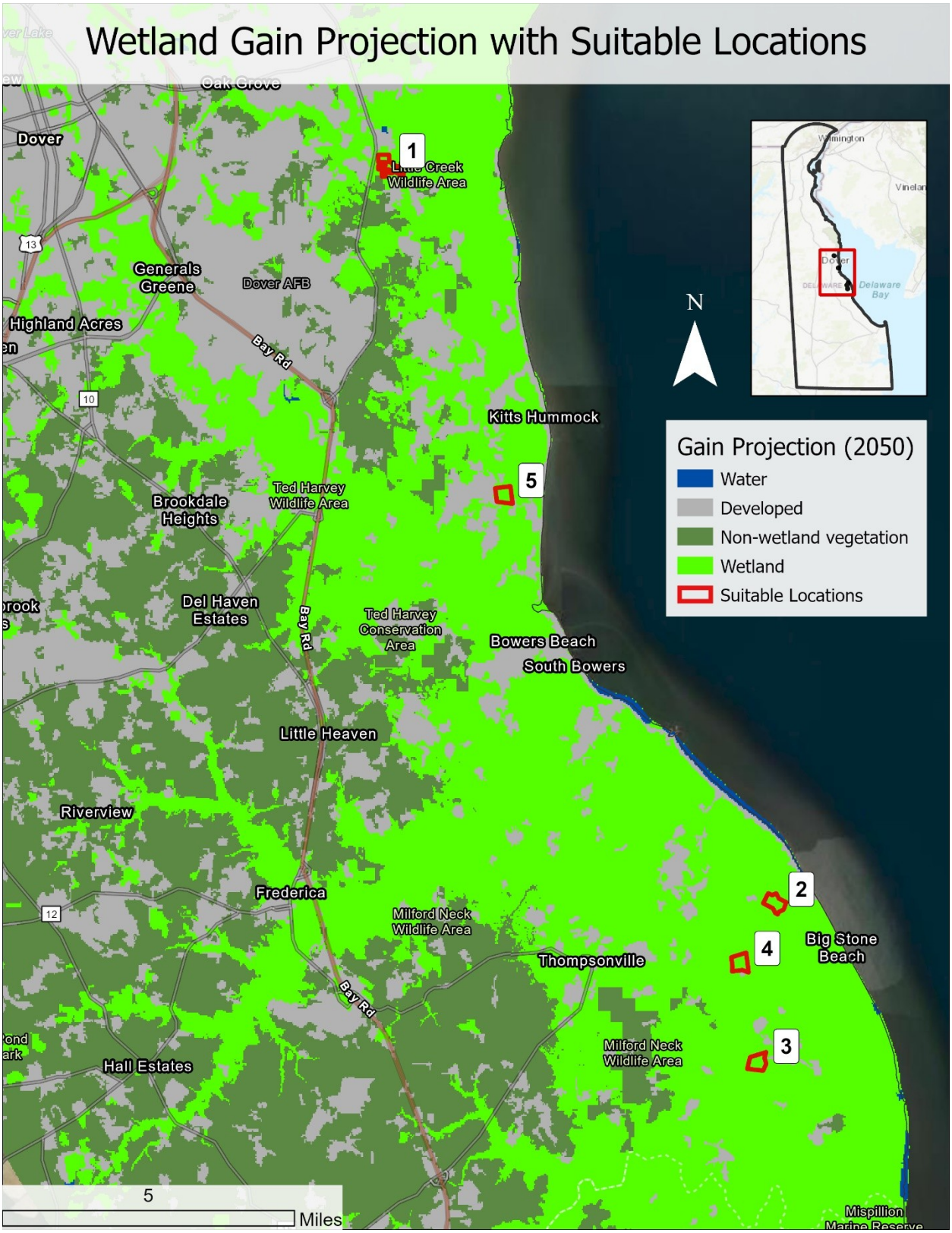

Figure B5. Top five suitable locations for marsh migration overlaid with the LULC change 2050 wetland gain projection.

Appendix C – Climate Analysis

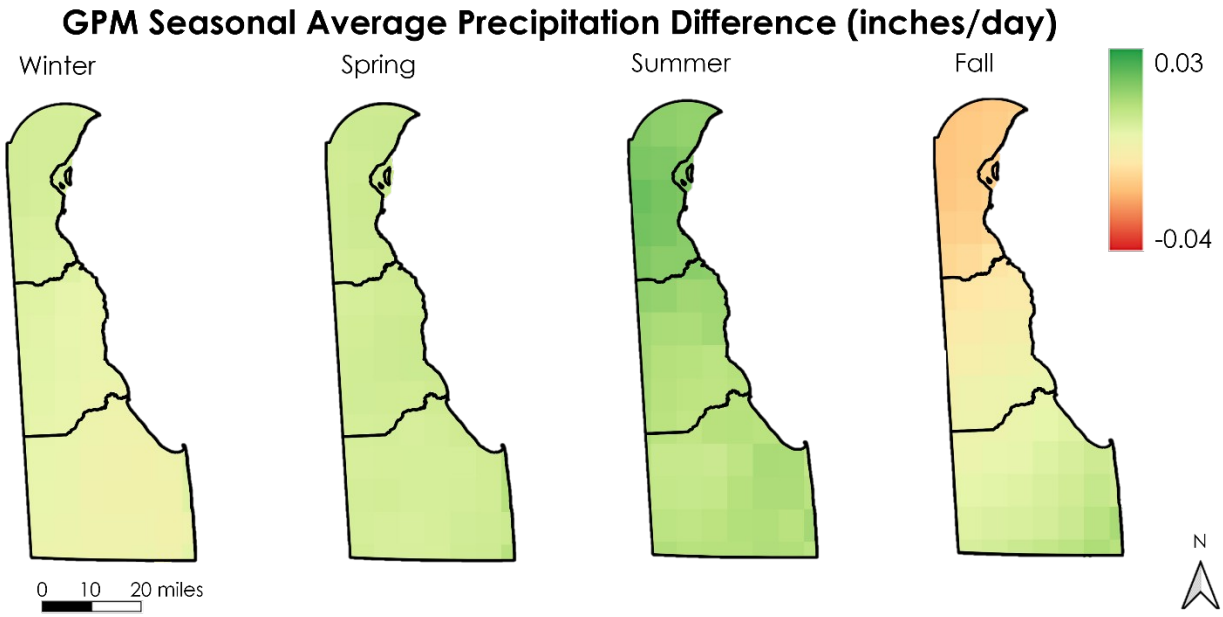

Figure C1. Difference maps of average seasonal precipitation change from 2000-2015 to 2015-2020.

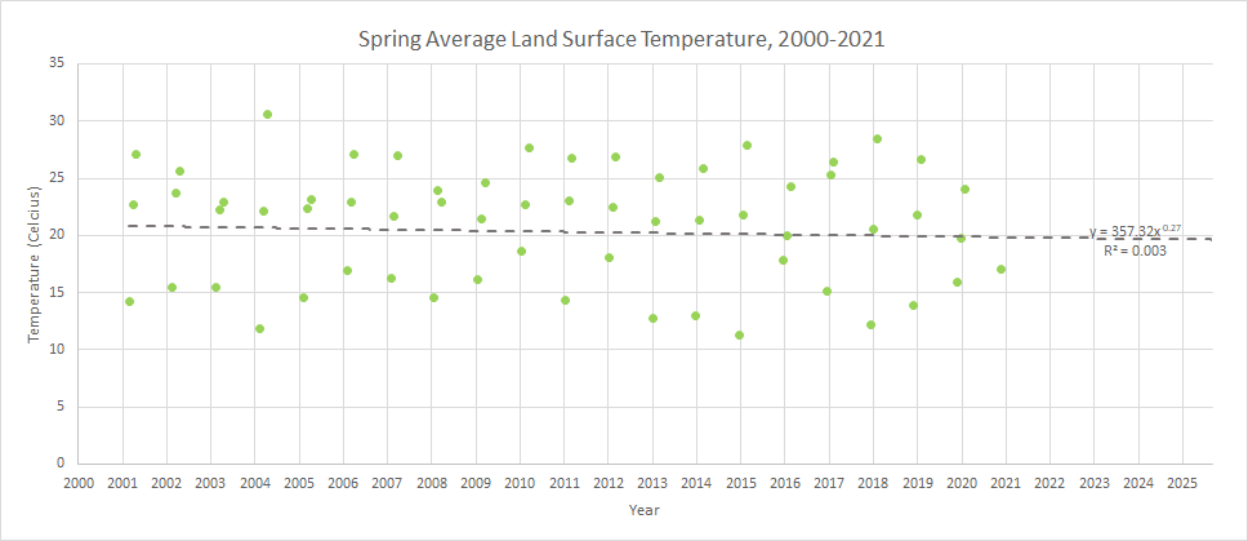

Figure C2. A scatterplot trend graph of seasonal average temperature across the state of Delaware for spring. The trend is represented by a Power Regression Trendline calculated using Microsoft Excel.

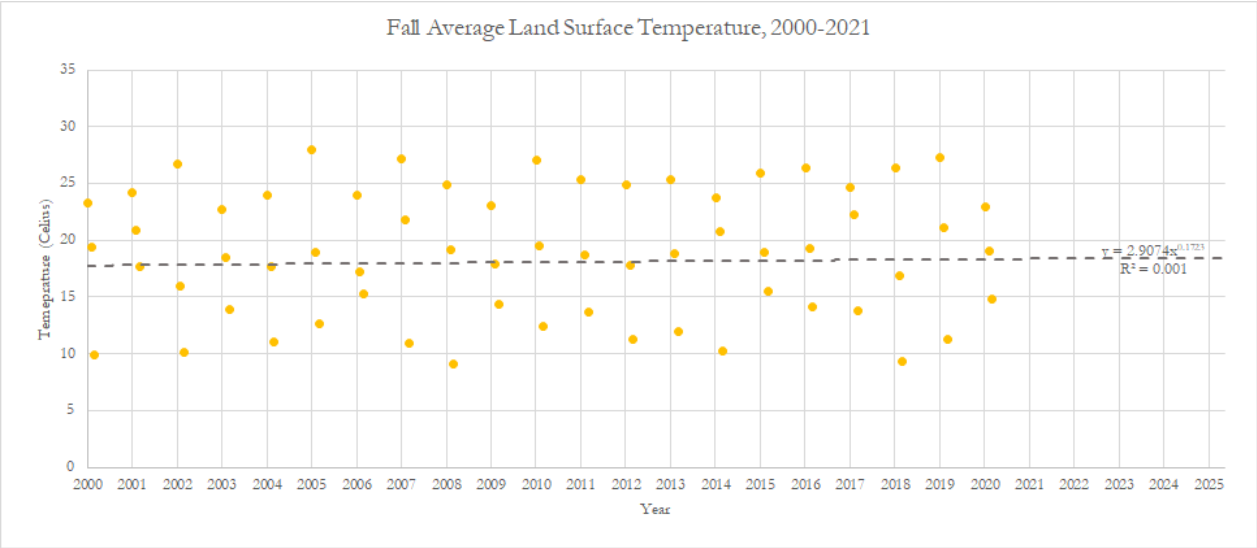

Figure C3. A scatterplot trend graph of seasonal average temperature across the state of Delaware for fall. The trend is represented by a Power Regression Trendline calculated using Microsoft Excel.

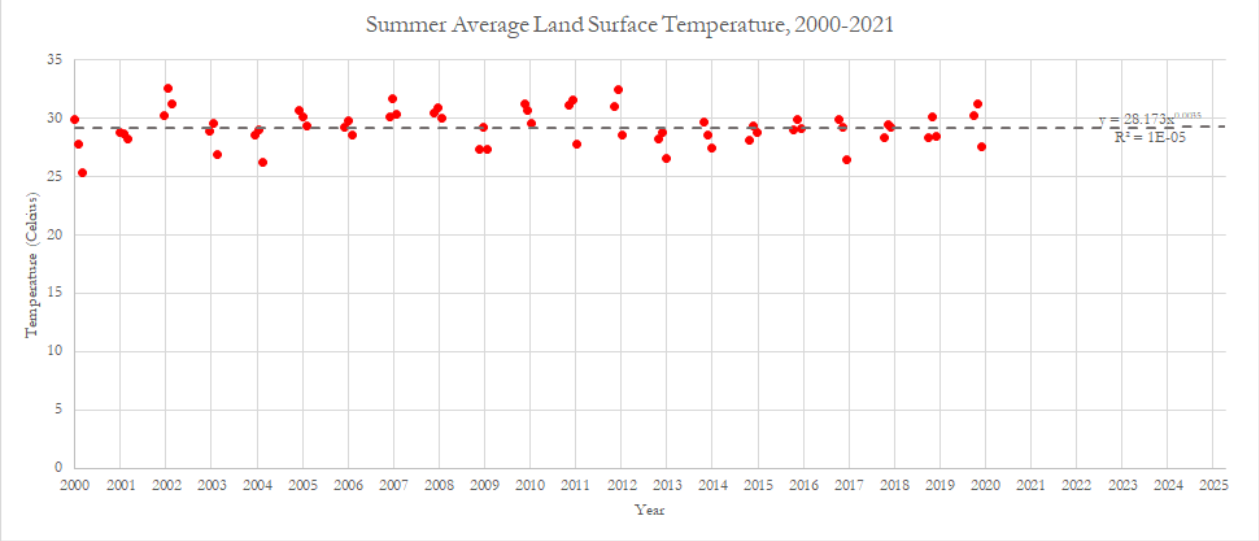

Figure C4. A scatterplot trend graph of seasonal average temperature across the state of Delaware for summer. The trend is represented by a Power Regression Trendline calculated using Microsoft Excel.

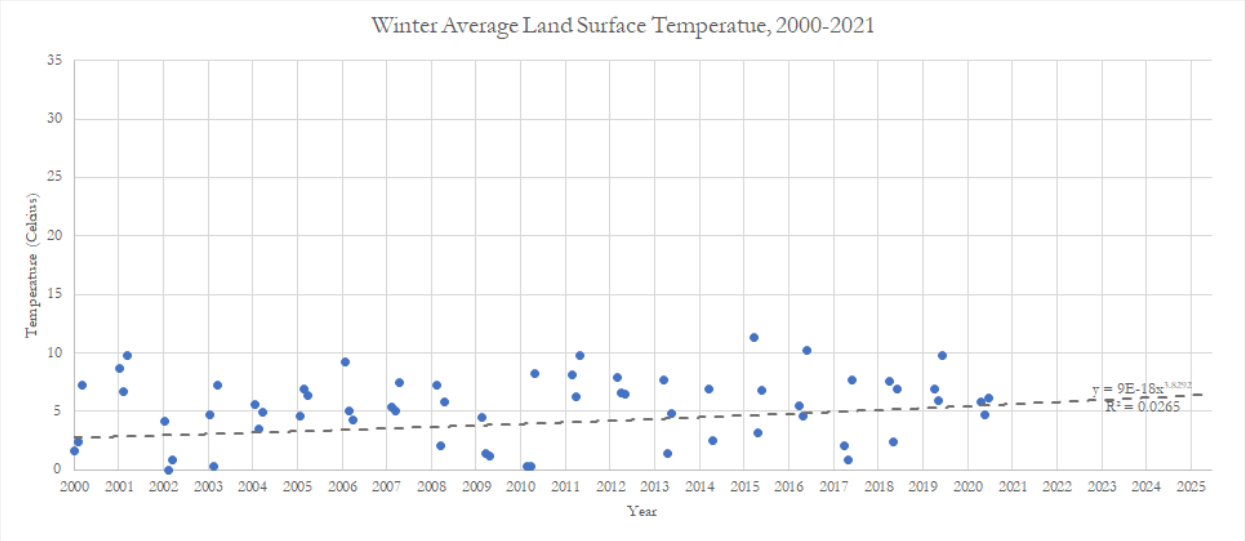

Figure C5. A scatterplot trend graph of seasonal average temperature across the state of Delaware for winter. The trend is represented by a Power Regression Trendline calculated using Microsoft Excel. One value was removed from this dataset (February 2015) due to the inability of the Power Regression to compute using negative values.

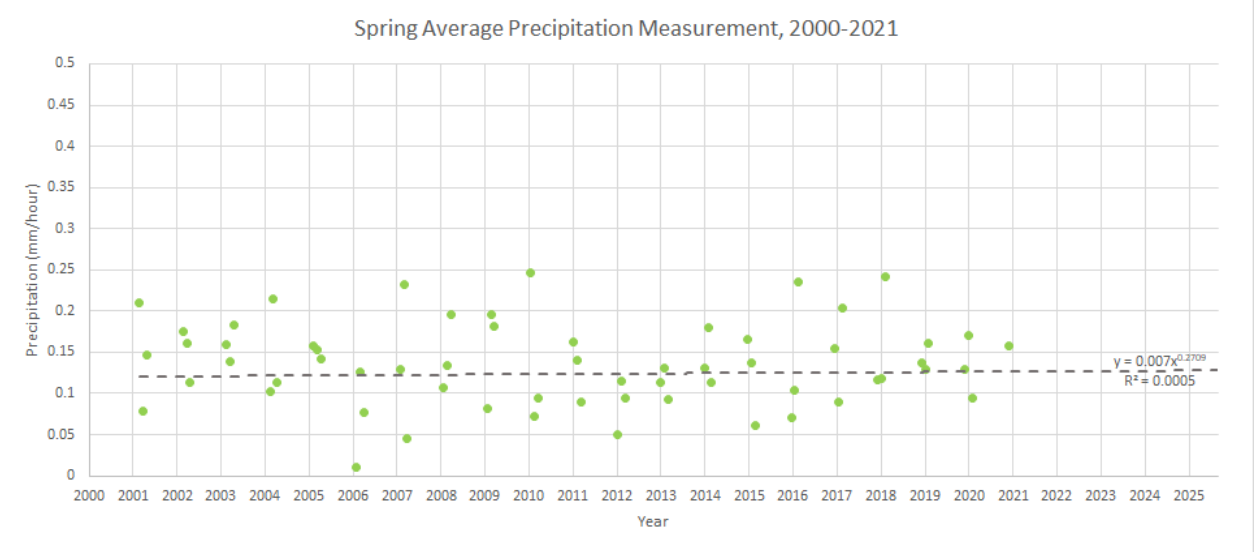

Figure C6. A scatterplot trend graph of seasonal average precipitation across the state of Delaware for spring. The trend is represented by a Power Regression Trendline calculated using Microsoft Excel.

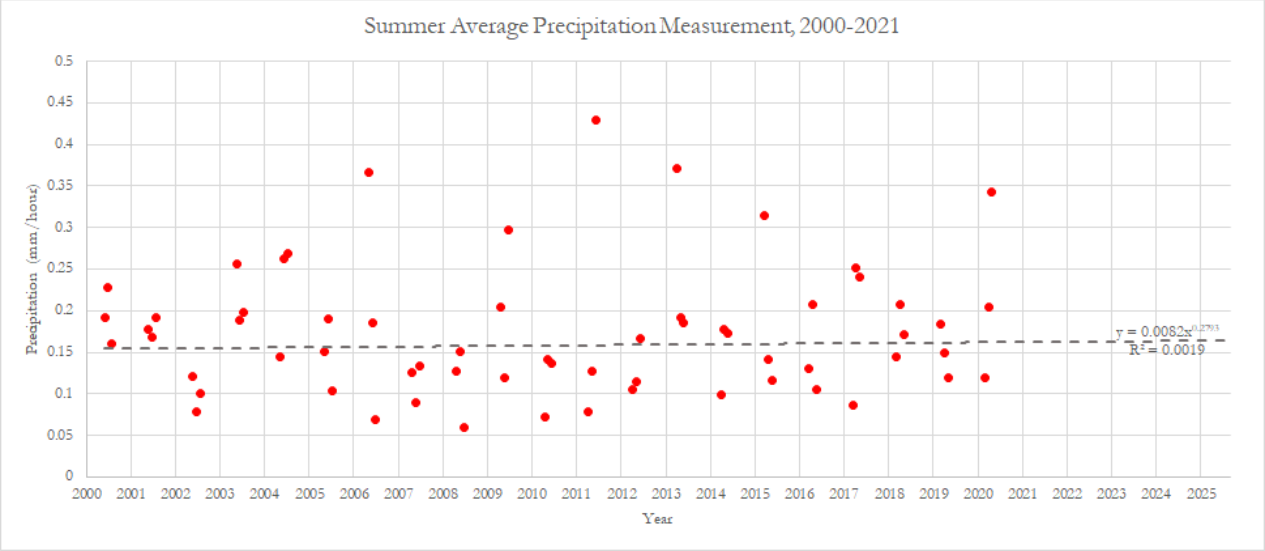

Figure C7. A scatterplot trend graph of seasonal average precipitation across the state of Delaware for summer. The trend is represented by a Power Regression Trendline calculated using Microsoft Excel.

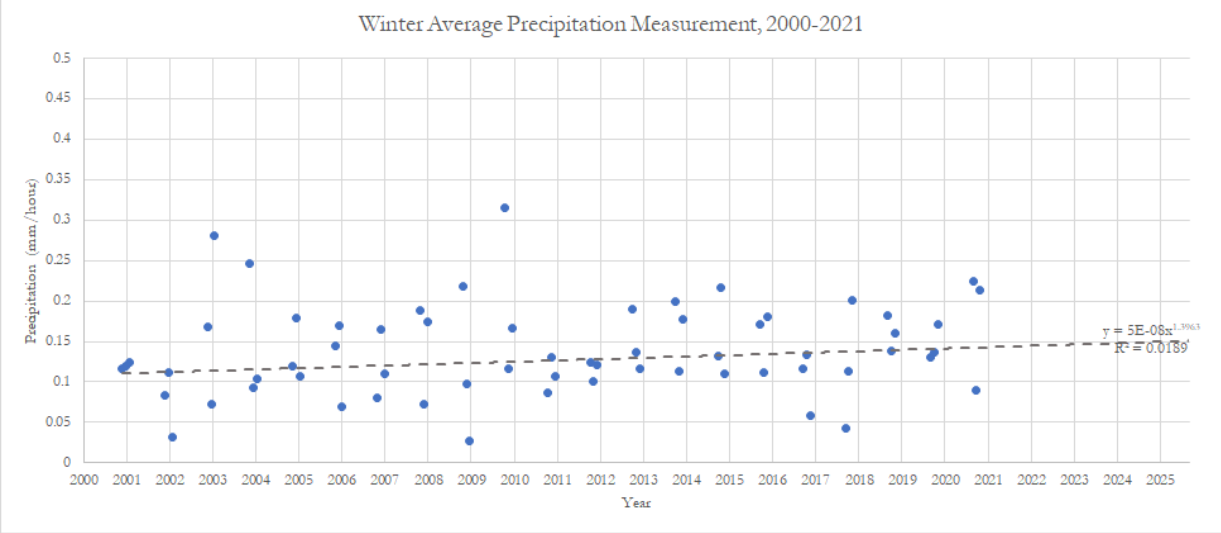

Figure C8. A scatterplot trend graph of seasonal average precipitation across the state of Delaware for winter. The trend is represented by a Power Regression Trendline calculated using Microsoft Excel.

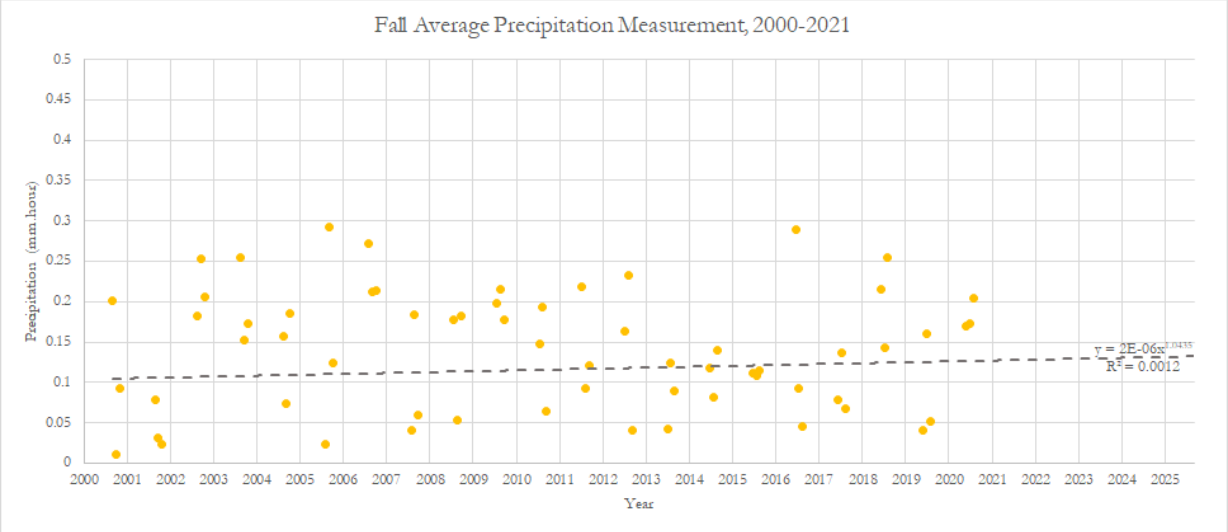

Figure C9. A scatterplot trend graph of seasonal average precipitation across the state of Delaware for fall. The trend is represented by a Power Regression Trendline calculated using Microsoft Excel.

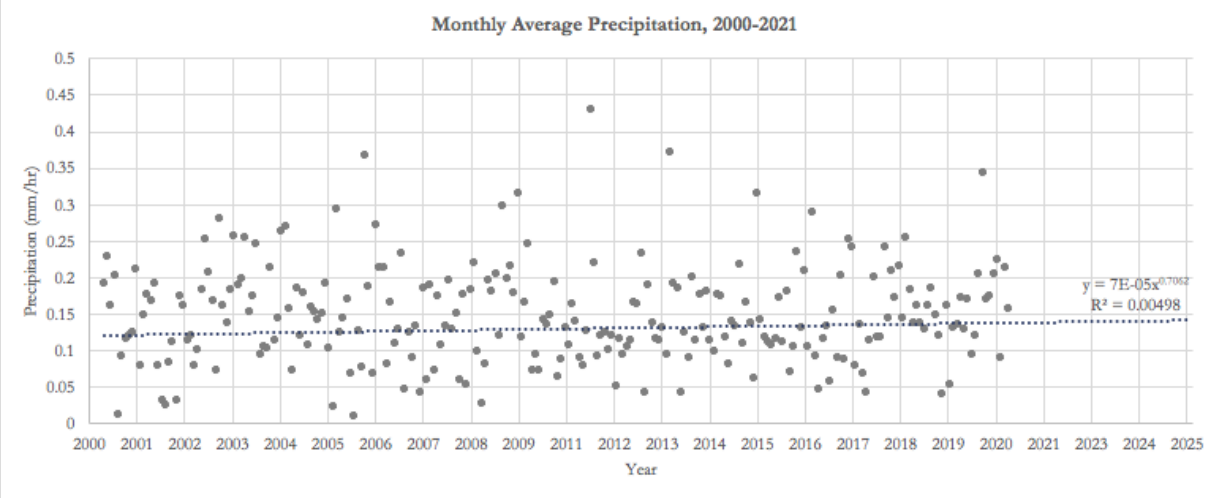

Figure C10. A scatterplot trend graph of monthly average precipitation (GPM) across the state of Delaware for each year. The trend is represented by a Power Regression Trendline calculated using Microsoft Excel.

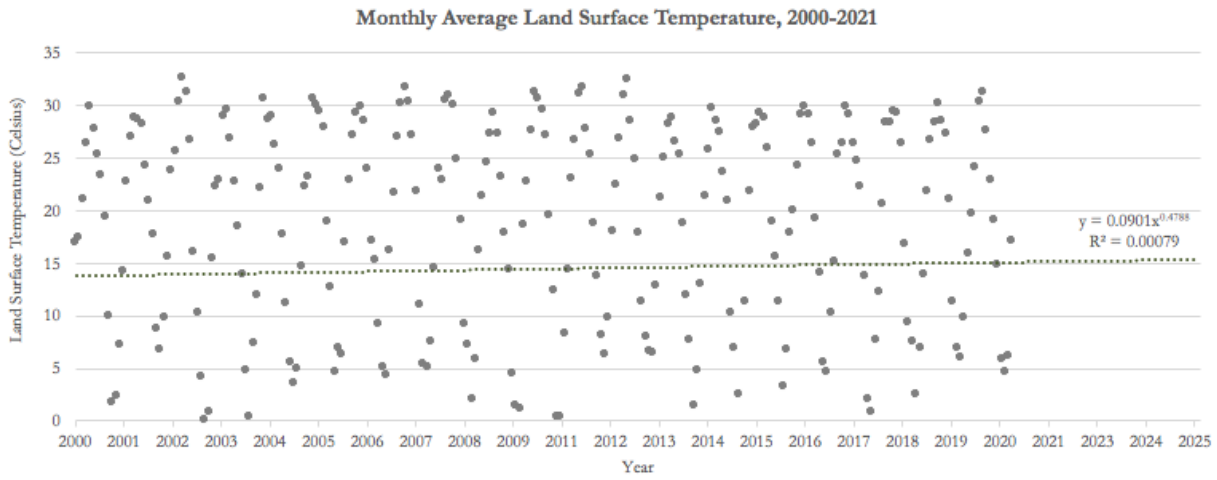

Figure C11. A scatterplot trend graph of monthly average land surface temperature (Terra MODIS) across the state of Delaware for each year. The trend is represented by a Power Regression Trendline calculated using Microsoft Excel.